NEUTRONIC FEASIBILITY ASSESSMENT OF FULL-CORE APPLICATIONS OF EVOLUTIONARY MIXED-OXIDE FUELS IN PRESSURIZED WATER REACTORS

by

Carrie J. Heitman

B.S., Nuclear Engineering
Massachusetts Institute of Technology, 1998

SUBMITTED TO THE DEPARTMENT OF NUCLEAR ENGINEERING IN PARTIAL FULFILLMENT OF THE REQUIREMENTS FOR THE DEGREE OF MASTER OF SCIENCE IN NUCLEAR ENGINEERING

AT THE

MASSACHUSETTS INSTITUTE OF TECHNOLOGY

FEBRUARY 1998

© 1998 Massachusetts Institute of Technology
All rights reserved.

Signature of the Author _____
Department of Nuclear Engineering
January 16, 1998

Certified by _____
Michael J. Driscoll
Professor Emeritus of Nuclear Engineering
Thesis Supervisor

Certified by _____
Stacey L. Eaton
Technical Staff Member, Los Alamos National Laboratory
Thesis Reader

Certified by _____
Paul Chodak III, Ph.D.
Technical Staff Member, Los Alamos National Laboratory
Thesis Reader

Accepted by _____
Lawrence M. Lidsky
Chairman, Department Comittee on Graduate Students

Science

NEUTRONIC FEASIBILITY ASSESSMENT OF FULL-CORE APPLICATIONS OF EVOLUTIONARY MIXED-OXIDE FUELS IN PRESSURIZED WATER REACTORS

by

Carrie J. Heitman

Submitted to the Department of Nuclear Engineering on January 16, 1998 in
Partial Fulfillment of the Requirements for the Degree of
Master of Science in Nuclear Engineering.

ABSTRACT

This thesis examines the performance of evolutionary mixed-oxide (EMOX) fuel in a standard Westinghouse PWR. EMOX is proposed as a tool for managing reactor grade plutonium inventories. The fuel is composed of reactor grade PuO_2, natural UO_2, and a ZrO_2-CaO matrix. Er_2O_3 is also used in some compositions as a homogeneous burnable neutron absorber. The inert, non-fertile ZrO_2-CaO component substitutes for specified amounts of the fertile UO_2 which would otherwise be present in standard mixed-oxide (MOX) fuel, and thus increases the plutonium destruction capability of the fuel. Several EMOX compositions with various PuO_2 loadings (3.0-6.0 vol.% total PuO_2), Er_2O_3 loadings (0.0-1.5 vol.%), and ZrO_2-CaO loadings (30-70 vol.%) are examined with regard to their reactivity behavior and their plutonium destruction capability.

A single assembly model of each composition was depleted through the equivalent of three 18 calendar month cycles, with each cycle being run at a different power level. The reactivity vs. burnup data at the beginning and end of each cycle were then used to define BOC and EOC power weighted core average reactivity (ρ_{core}) values for comparison with appropriate maximum and minimum criteria. Fuel compositions which were able to meet the BOC and EOC reactivity criteria were recommended for further study. None of the 3.0 vol.% PuO_2 cases or the 0.0 vol.% Er_2O_3 cases were acceptable. Of the remaining compositions , at least one was selected at each PuO_2, ZrO_2-CaO, and Er_2O_3 loading. The reactivity vs. burnup behavior of the selected EMOX cases compares favorably with that of UO_2 fuel.

The plutonium destruction capability of EMOX is shown to exceed that of MOX in all cases. Plutonium destruction is increased as more non-fertile material is used in the fuel. The isotopic content of plutonium in the spent EMOX fuel is also favorably affected by higher ZrO_2-CaO loadings in that the ratio of non-fissile to fissile plutonium is increased. From the results of this preliminary investigation, EMOX appears to be a viable alternative to standard MOX fuels. It is noted, however, that much work remains to be done in characterizing this fuel form, and specific issues requiring elaboration are identified.

Thesis Supervisor: Michael J. Driscoll
Title: Professor Emeritus of Nuclear Engineering

Thesis Reader: Stacey L. Eaton
Title: Technical Staff Member, Los Alamos National Laboratory

Thesis Reader: Paul Chodak III
Title: Technical Staff Member, Los Alamos National Laboratory

ACKNOWLEDGMENTS

I owe a great deal to my thesis supervisor, Prof. Michael J. Driscoll, and to my thesis readers, Stacey L. Eaton and Dr. Paul Chodak III. I am very grateful for their infinite patience and for all of the guidance which they have given me during this work.

I would also like to thank the many people in group TSA-10 at Los Alamos National Laboratory (LANL) who aided me in carrying out my research there. Specifically, John Buksa, Dr. Russell D. Mosteller, and Russell Johns were of great help to me as I outlined this project and develped a HELIOS assembly model.

This study was funded with LANL internal funds as part of the Laboratory Directed Research and Development project.

Finally, I would like to thank Matthew Gray for his wide ranging contributions. Without his love, support, and computer skills, I might never have completed this thesis.

TABLE OF CONTENTS

LIST OF FIGURES

LIST OF TABLES

CHAPTER ONE: INTRODUCTION

1.1 Objectives

The existence of large and growing inventories of reactor grade plutonium (RGP) worldwide has drawn the concern of some members of the scientific community [N-1]. This work investigates a new reactor fuel form, evolutionary mixed-oxide (EMOX), which is designed to be a flexible RGP inventory management tool. Several EMOX compositions are examined for basic compatibility with current commercial pressurized water reactor (PWR) cores and operational constraints. A model of a standard Westinghouse PWR assembly is used to simulate a full core loading of each composition as it is burned through three 18-month cycles . The performance of the fuels is judged via power-weighted reactivity integrals, reactivity versus burnup behavior, and end of life (EOL) plutonium (Pu) content . EMOX results are also compared with those of standard uranium fuel. The goal of this investigation is to determine which EMOX compositions are promising candidates for use in commercial PWRs and to suggest areas in which future work on these fuels is needed.

1.2 Motivation and Background

Much attention has been given to the question of how to disposition up to 50 metric tons (MT) of weapons grade plutonium (WGP) which may be declared in excess of United States (US) military needs over the course of the next several years [N-1]. Likewise, there is concern over the fate of equal or greater amounts of excess WGP which may result from dismantlement activities in the Former Soviet Union. One of the major concerns regarding this material is the possibility that it might someday be reused to create nuclear weapons. Members of the expert community have concluded that this is a wholly valid concern [N-1]. This material is comprised mostly of plutonium-239, which decays with a 24,000 year half life. If the plutonium is not destroyed via some form of transmutation, most likely fission, it will need to be physically protected into the far distant future in order to insure that it is not refabricated into a weapon. In view of these circumstances, the US has spent a great deal of time and money to investigate WGP disposition options.

There is a much larger quantity of plutonium, however, which has been given much less attention. Over 800 MT of unseparated plutonium existed worldwide in nuclear reactor spent fuel as of 1996 [A-2]. This material is known as reactor grade plutonium because it is created through the high burnup irradiation of uranium fuels, and its isotopic composition differs markedly from that of WGP. It typically contains approximately 60% Pu-239. RGP is not as well suited as WGP for creating nuclear weapons, but it could be used to make a crude nuclear explosive, and hence poses a potential proliferation threat [C-1]. Inventories of RGP are ever increasing, and as worldwide quantities continue to grow, so do the difficulties associated with safeguarding this material. These considerations have prompted members of the scientific community to pursue technologies which would allow RGP inventories to be controlled.

One such technology is irradiation of the plutonium in a nuclear reactor. Several new fuel forms have been proposed for this task [P-2, O-2, C-1]. These fuels are intended

to allow plutonium to be burned in existing light water reactors (LWRs). One motivation for investigating novel LWR fuel designs is the fact that LWRs are the most prevalent kind of nuclear reactors in operation today. This type of reactor, therefore, has the greatest potential to affect the global inventory of RGP. Additionally, fuels which can be burned in existing reactors without substantial hardware changes will theoretically require less development before being licensable.

Mixed-oxide (MOX) fuel, which is composed of urania (UO_2) and plutonia (PuO_2) has been used in Europe to recycle some of the RGP created in its commercial reactors. The use of MOX fuel has the potential to destroy more plutonium than it breeds. However, in the typical one-third-core MOX configurations currently used in Europe, core-averaged plutonium inventories actually increase due to the large amounts of fertile uranium-238 in the core. Larger MOX core loadings can result in net plutonium destruction, but they may push the envelope of reactor safety and control constraints [O-1]. Various fuels which do not contain uranium, and therefore do not breed plutonium, have been proposed, such as thoria-plutonia (PuO_2-ThO_2) and plutonia-zirconia (PuO_2-ZrO_2). Preliminary investigations indicate they are capable of destroying large fractions (greater than 60%) of the plutonium they initially contain [S-1]. Non-fertile fuels (NFFs) differ in significant ways from UO_2, however, and would require extensive development and testing before they could be used on any significant scale [C-1]. The eventual development of such fuels offers the possibility of nearly complete destruction of plutonium inventories. However, a fuel option which could offer greater plutonium destruction than standard MOX, yet be more easily licensed than NFF, could be useful for bringing plutonium production under control in the near term. This work proposes such a fuel form and explores its performance as compared to UO_2 and MOX fuels.

The EMOX program at Los Alamos National Laboratory (LANL) began as part of a study of a NFF concept first investigated at Idaho National Engineering and Environmental

Laboratory (INEEL). The INEEL work was prompted by the National Academy of Sciences (NAS) Committee on International Security and Arms Control (CISAC) to assess the potential of several different nuclear fuels to burn surplus US WGP [S-1]. Among several oxide fuels they examined, the plutonia-zirconia-calcia-erbia (PuO_2-ZrO_2-CaO-Er_2O_3) fuel form showed the most promise as a candidate for use in LWRs. This fuel composition was examined more closely in an additional INEEL study and was also chosen for further investigation at LANL [S-2]. While the INEEL studies focused on WGP disposition, investigators at LANL became more interested in the problem presented by RGP stockpiles. As previously mentioned, however, it was quickly apparent that the NFF concept would require extensive research and development before it could be licensed for commercial LWR use.

EMOX was then conceived as a way to provide a more gradual transition between MOX and NFF. EMOX incorporates UO_2 and PuO_2, like standard MOX, but also contains a non-fertile component composed of ZrO_2-CaO. This non-fertile component displaces some of the uranium in the fuel which would otherwise breed additional plutonium. Er_2O_3 may also be used in EMOX as a depletable neutron absorber. EMOX compositions containing small amounts of non-fertile material are expected to be more easily licensed than fully NFF. These compositions will be very similar to MOX and may, therefore, be able to draw on the extensive database which already exists. Progressively higher content non-fertile EMOX compositions could, likewise, create a path towards the eventual use of fully non-fertile fuels.

EMOX has the advantage of potentially being able to accommodate many different plutonium management scenarios. Varying the percentage of the EMOX fuel volume which is occupied by each of its four components (PuO_2, UO_2, ZrO_2-CaO, Er_2O_3) allows the amount of plutonium in the resulting spent fuel to be controlled. Large amounts of plutonium could be destroyed quickly through the use of high non-fertile and plutonium

loadings, whereas lower loadings should allow plutonium inventories to decrease more slowly. Once plutonium stores reach an acceptable level, an EMOX composition could be tailored to maintain that inventory. Compositions with low plutonium and non-fertile loadings could even be used to slowly breed plutonium.

Previous work supports the use of a calcium-stabilized zirconium oxide inert matrix in LWR fuel as well as the choice of erbium as a depletable neutron absorber for use with plutonium, uranium (U), and MOX fuels. There is NFF work, in addition to that of INEEL, which concluded that zirconia and erbium are the inert matrix and depletable neutron absorber of choice for a plutonium fuel [C-1]. Irradiation experience with UO_2-ZrO_2-CaO fuel has demonstrated that it performs very similarly to standard uranium fuel, and the addition of small amounts of plutonium to this fuel is not expected to greatly alter this result [B-1, S-1]. Also, erbia has been recommended for use in PWR fuels, including uranium and MOX fuels [J-1, C-2, L-1].

1.3 Preview and Structure of this Report

This work is a preliminary evaluation of the performance of various EMOX fuel compositions in a typical Westinghouse 4-loop PWR. A full core EMOX loading was simulated via a single assembly model which was burned through three 18-month equilibrium cycles. Each cycle was run at a different power level to imitate the experience of an assembly as it is placed in three different core locations during its lifetime. Calculations were done using the HELIOS code developed by Scandpower after the code was benchmarked for accuracy in both its criticality and isotopic depletion calculations [C-3].

Three parameters characterizing fuel composition were varied in this performance survey. The percentage of the fuel volume (vol.%) which was comprised of ZrO_2-CaO is

referred to as the non-fertile percentage (NFP) of the fuel. Compositions having NFPs of 30, 50 and 70 were examined. At each of these NFPs, PuO_2 and Er_2O_3 loadings were also varied. PuO_2 levels of 3, 4, 5, and 6 vol.% were studied while Er_2O_3 loadings of 0.0, 0.5, 1.0, and 1.5 vol.% were examined. The percentage of each fuel composition which was not devoted to ZrO_2-CaO, PuO_2, or Er_2O_3 consisted of natural UO_2.

The performance of the EMOX fuels has been judged in a number of ways. A standard Westinghouse uranium fuel assembly which incorporates erbium as a depletable neutron absorber served as a baseline for comparison with the EMOX cases. The reactivity behavior, as a function of burnup of the EMOX compositions, was compared with that of the uranium assembly. Also, beginning of cycle (BOC) and end of cycle (EOC) average core reactivities were calculated, to verify that EMOX cores could remain critical and not exceed reactivity limits. The amount and isotopic composition of the plutonium contained in the spent EMOX fuel has been closely examined. The Pu destruction of MOX assemblies containing 3-6 vol.% PuO_2 was compared to that of EMOX. Finally, a few promising EMOX compositions were run using CASMO-3 to verify results of interest [E-1].

The following chapter (Chapter Two) will go into more detail about the codes, benchmarks, and model specifications which were used in this work. Chapter Three of the thesis will present the results obtained from the EMOX calculations. Finally, Chapter Four will discuss conclusions which can be drawn and propose future work.

CHAPTER TWO: METHODOLOGY

2.1 Introduction

This chapter provides details regarding the calculations performed for this work and the computer codes which were used. First, the HELIOS code, previously performed benchmarks, and applications of the code are described. Benchmark calculations which were performed as part of this work are then discussed. The HELIOS assembly model used to evaluate EMOX compositions against a uranium fuel composition is described. Finally, CASMO-3 EMOX calculations used to confirm certain HELIOS results are presented.

2.2 HELIOS Description

Version 1.3 of the HELIOS code by Scandpower was used in this work to perform burnup and criticality calculations. HELIOS is a two-dimensional collision probability based transport code, capable of supporting general geometries. The code also has the capability to use cosine coupling at the interfaces between sub-systems in order to allow savings in computational time. Depletion calculations are performed using a cross-section library containing 270 materials and 115 fission products. The library is divided into 34

energy groups and is based on ENDF/B-VI, release two, data. Data is included on most materials between 300 and 1200 K, but fuel material data is available up to 2000 K.

The HELIOS code is run in conjunction with two additional codes: AURORA, an input processor, and ZENITH, an output processor. An AURORA input deck includes all of the specifications of desired calculations, including geometry, materials information, power levels, size and number of burnup steps, etc. AURORA processes the input deck and writes the resulting information to a data base file which is referred to as a HERMES file. HERMES is a set of subroutines which maintains and accesses the data base in response to the needs of AURORA, HELIOS, and ZENITH. After AURORA has created a data base, HELIOS can be run and will in turn write its results to the data base. A ZENITH input file, which specifies the desired output and output format, must then be created. Finally, running ZENITH will produce an output file which contains all of the requested calculational results.

HELIOS has been benchmarked and applied by previous investigators. Ilas and Rahnema benchmarked HELIOS with the 34-group ENDF/B-VI-based library against MCNP4A with a continuous energy ENDF/B-VI library [I-1]. They modeled a BWR pin cell with UO_2 fuel of different enrichments and, in some cases, poisoned by gadolinium. K_{eff} values and Doppler and void coefficients of reactivity were calculated. They concluded that HELIOS' Doppler and void coefficients were in good agreement with those from MCNP. Differences between the k_{eff} values from the two codes increased with fresh fuel enrichment, leading them to conclude that the HELIOS absorption cross sections for U-235 are probably somewhat overestimated.

Kim and Yoon used HELIOS in a parametric feasibility study of a deuterium moderated pressurized light water reactor [K-1]. They modeled CANDU-like fuel assemblies with surrounding double pressure tubes. The inner tubes contained enriched UO_2 fuel and light water coolant while the outer tubes held D_2O for moderation. Coolant,

moderator, and void coefficients were calculated as a function of burnup for various fuel to coolant ratios and moderator thicknesses. The study concluded with the selection of a specific fuel enrichment and geometry.

Previous EMOX investigations have also been done at LANL using HELIOS. Eaton et. al. developed a HELIOS PWR pin cell model and performed depletion calculations to determine the plutonium destruction capability of fractional-core EMOX loadings [E-2]. MOX and non-fertile fuels were also simulated as comparison cases. The study concluded that EMOX has the potential to be an effective plutonium management tool. The present work is a further investigation of this potential.

As noted in Section 3.2.3, there are sufficient differences in reactivity and plutonium isotope concentrations at EOL between HELIOS and CASMO-3 results for the same assembly calculation to warrant further intercomparisons. Since there are basically no experimental benchmarks at high non-fertile percentages, further comparisons against MCNP are also in order.

Finally, an automated procedure for combining HELIOS with a whole-core few group code must be developed if investigations of the present sort are to go beyond the scoping study level.

2.3 Benchmark Calculations

Critical experiment data and previously performed CASMO-3 calculations were used to benchmark the HELIOS code's criticality and isotopic depletion calculations, respectively. This section will first present a calculational benchmark performed against a series of critical lattice experiments and then describe a pin cell isotopic benchmark.

2.3.1 Critical Benchmark. Critical experiments conducted by Pacific Northwest Laboratories (PNL) were used as criticality benchmarks [C-4]. These experiments (PNL

30-35) were light-water moderated MOX fuel pin lattices with three different pitches. Two trials were performed at each pitch, one with a borated moderator and one without boron. For the borated moderator trials, criticality was achieved by reducing the soluble boron concentration. For trials with unborated moderators, fuel pins were added to achieve criticality. The MOX fuel contained 2 wt% PuO_2. Table 2.1 shows the fuel composition and pin cell dimensions as given in the benchmark specifications and as used in HELIOS models of the PNL cases. Figure 2.1 displays the spatial mesh which was used in modeling each of the PNL pin cells. Only two fuel and five coolant regions were used as a compromise between accuracy and computational resource requirements.

Table 2.1 PNL Pin Cell Specifications

Region	Outer Radius (cm)	Isotope	Concentration (10^{24} atoms/cm^3)
Fuel	0.6414	Pu-239	3.974×10^{-4}
		Pu-240	3.344×10^{-5}
		Pu-241	1.600×10^{-6}
		Pu-242	1.200×10^{-7}
		U-235	1.504×10^{-4}
		U-238	2.073×10^{-2}
		O-16	4.401×10^{-2}
Clad	0.7176	Zr_{nat}	4.226×10^{-2}
Moderator	(see Table 2.2)	H-1	6.671×10^{-2}
		O-16	3.336×10^{-2}
		B-10	(see Table 2.2)

Figure 2.1 HELIOS Model of PNL Pin Cell

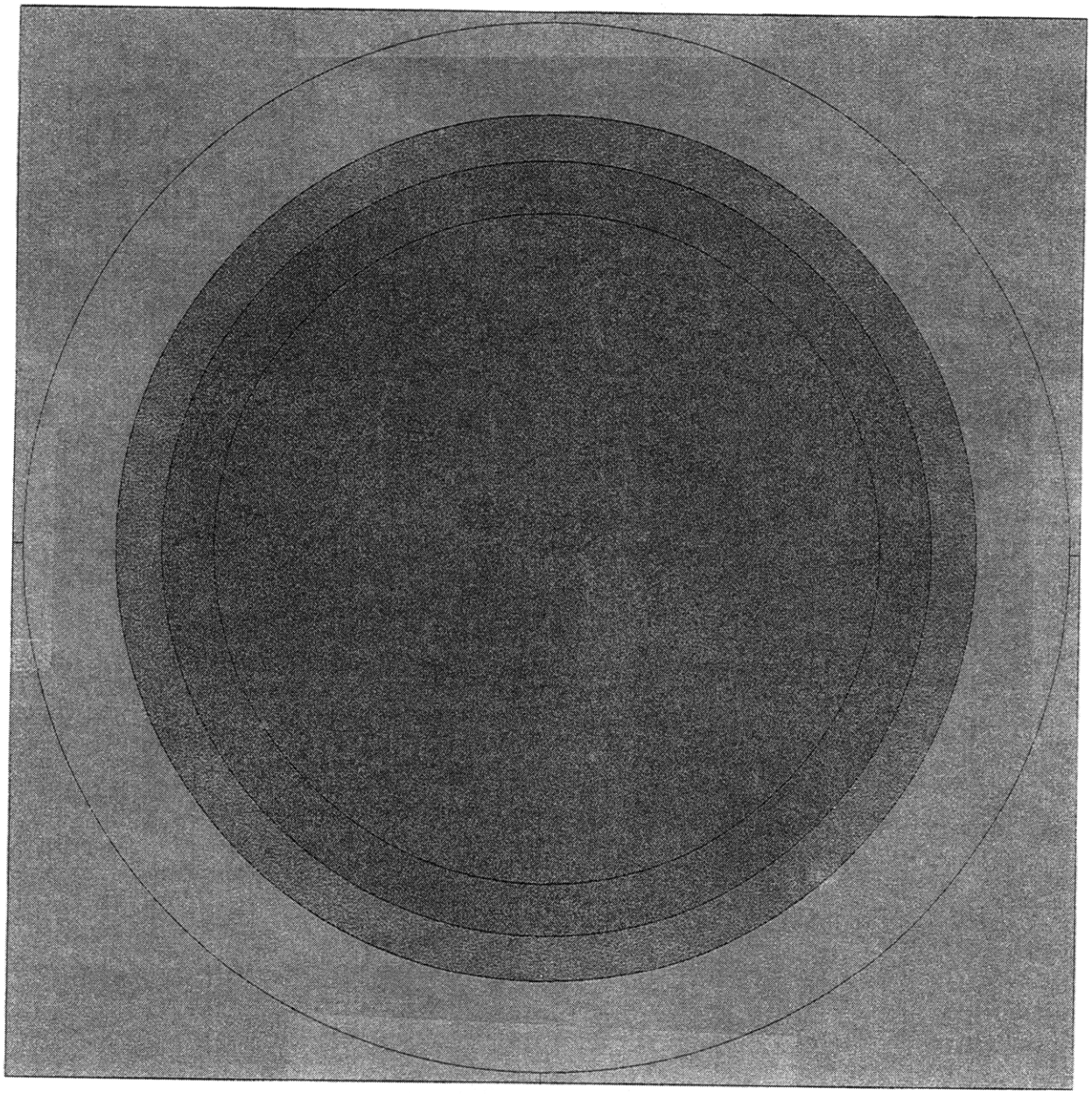

The two darkest inner circles are the fuel regions. The next, slightly lighter circle represents the clad/gap, and the outermost five regions are moderator regions. The pin pitch (linear dimension of the square cell) varies from 1.778 to 2.51447 cm depending upon which PNL case is being modeled.

Table 2.2 lists important lattice parameters for the various experiments. The moderator temperatures given were applied to all of the materials in the lattices for lack of knowledge of specific fuel and cladding temperatures. The experimental lattices were all reported to be slightly supercritical as can be seen from the measured k-effective (k_{eff}) values. Plutonium-oxide particle effects present in the experiments are mentioned, but not explained, in the benchmark specifications. It was assumed that the corrections were meant to account for self-shielding effects due to MOX particle size.

In the PNL experiments, the fuel pins were held in place by two aluminum "egg crate" structures, one near the top of the lattice and one near the bottom. An aluminum slab supported the pins from underneath, and there was a lead shield resting on top of the core. More than 20 cm of water reflected the sides and bottom of the core, but the top reflectors ranged between 2 and 16 cm in thickness. The three-dimensional experiments were modeled with HELIOS' two-dimensional capability using axial buckling values taken from experimental measurements [S-3]. The HELIOS benchmark model simulates a horizontal slice through the middle of the core, and therefore contains only the fuel pins themselves and the water moderator and reflector.

Figure 2.2 shows the HELIOS model of the PNL-30 case. The HELIOS models for cases PNL-31 through 35 can be found in Appendix B. All of the cases, with the exception of PNL-32, were octant symmetric and were simulated using eighth-core models with reflective radial boundary conditions. PNL-32 had no core symmetry and was fully modeled. PNL-33 and PNL-31 had the same pin arrangement . The water reflectors are all greater than 20 cm thick and considered to be neutronically infinite. Therefore, black outer water boundary conditions were used. The exact geometry used in all HELIOS benchmark calculations can be inferred from the HELIOS input files. These can be obtained from Prof. M. J. Driscoll of the MIT Nuclear Engineering Department.

Table 2.2 PNL Lattice Parameters

Case	Pitch (cm)	Boron-10 Concentration (10^{24} atoms/cm^3)	Moderator Temperature (°C)	Axial Buckling (cm^{-2})	Critical Number of Pins	Experimental k-effective	Δk_{eff} for PuO_2 Particle Effects
PNL-30	1.77800	1.873×10^{-8}	21	0.0009091	469	1.00017	0.0
PNL-31	1.77800	7.504×10^{-6}	22	0.0009381	761	1.00006	0.0
PNL-32	2.20914	9.916×10^{-9}	23	0.0009322	195	1.00028	-0.0018
PNL-33	2.20914	1.202×10^{-5}	23	0.0009487	761	1.00023	-0.0018
PNL-34	2.51447	1.763×10^{-8}	22	0.0009842	161	1.00077	-0.0025
PNL-35	2.51447	8.455×10^{-6}	23	0.0009480	689	1.00013	(-)0.0025

Figure 2.2 HELIOS Model of Lattice PNL-30

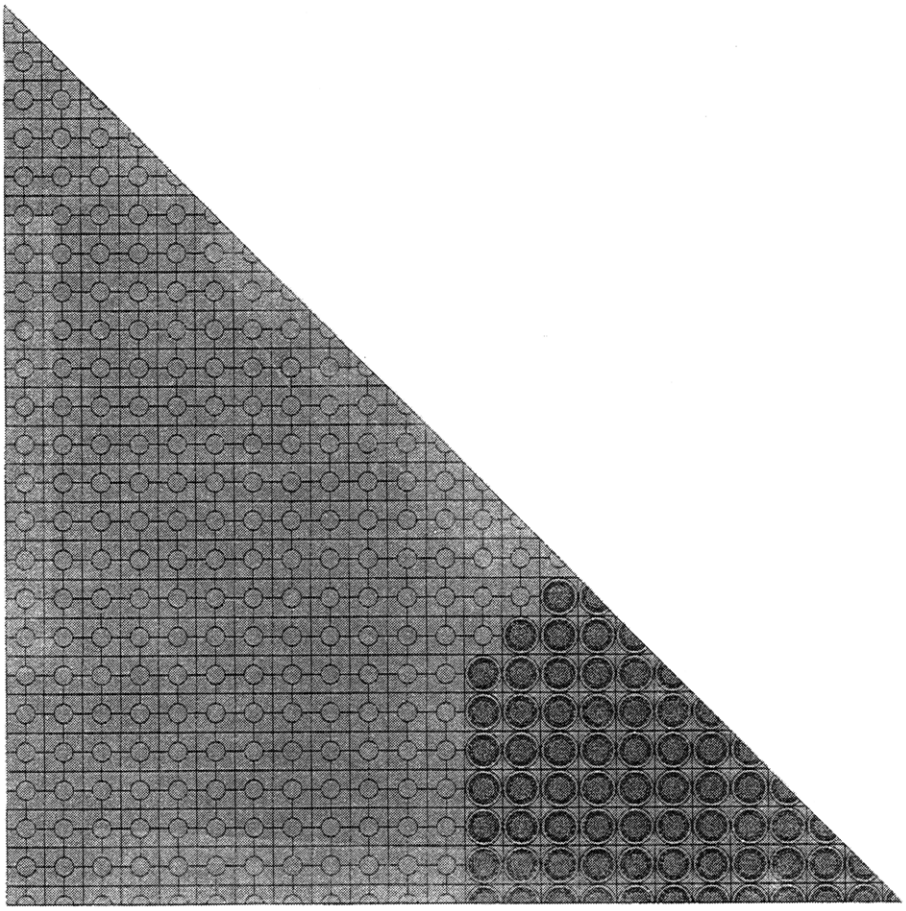

Squares containing dark inner circles are fuel pin cells. All other squares are moderator regions (divided into five subregions). The figure is drawn to scale. One inch on the page represents 9.09 cm.

Table 2.3 gives k_{eff} results obtained from the HELIOS benchmark calculations, and compares them to the corrected experimental k_{eff} values. The calculated k-effectives are all within ± 0.008 of the benchmark values with the exception of PNL-35, which differs by 0.01337. These results are within the likely uncertainty of the experimental values reported in the benchmark specifications. In view of this, HELIOS is believed to be capable of performing sufficiently accurate criticality calculations on plutonium-containing fuel lattices.

Table 2.3 PNL Benchmark Results

Case	Benchmark k_{eff}	HELIOS k_{eff}	Difference
PNL-30	1.00017	0.99999	0.00018
PNL-31	1.00006	0.99797	0.00209
PNL-32	0.99848	0.99873	-0.00025
PNL-33	0.99843	1.00640	-0.00797
PNL-34	0.99827	0.99660	0.00167
PNL-35	0.99763	1.01100	-0.01337

2.3.2 Isotopic Benchmark. A single UO_2 pin cell depletion calculation was performed as an isotopic benchmark. The specifications for the pin cell and the results given by CASMO-3 for the depletion calculation were taken from a benchmark by Chodak [C-1]. The specifications used in his work were originally published in an EPRI report [F-1], however, no isotopic benchmarks were associated with that report.

The HELIOS model used in this case was similar in configuration to Figure 2.1, but its fuel region contained eight regions in order to increase the accuracy of the depletion calculations. The EPRI-defined pin cell contains uranium fuel and has a borated light water moderator. The model dimensions, temperatures, and materials are listed in Table 2.4. The outer moderator boundary of the cell was completely reflected so as to simulate an

infinite lattice. A specific power of 43.72 W/g heavy metal was used in irradiating the pin to 36 GWd/MT.

Table 2.4 EPRI Pin Cell Specifications

Region	Outer Radius (cm)	Temperature (K)	Isotope	Concentration (10^{24} atoms/cm^3)
Fuel	0.41169	922.04	U-234	7.17941×10^{-6}
			U-235	8.93440×10^{-4}
			U-238	2.17301×10^{-2}
			O_{nat}	4.52432×10^{-2}
Clad	0.47587	614.04	Zircaloy-2	3.87351×10^{-2}
Moderator	Pitch: 1.25984	572.04	H-1	4.87183×10^{-2}
			O-16	2.43608×10^{-2}
			B-10	4.01063×10^{-5}
			B-11	1.62861×10^{-5}

The results of the depletion calculations are presented in Table 2.5. The number densities produced by HELIOS and CASMO were converted to weight percentages based on the total mass of the nuclides presented in the table. Comparisons are made at 1, 5, 16, and 36 GWd/MT. The discrepancies between the two codes grows consistently with burnup. At 36 GWd/MT, U-238 and Pu-239 show the largest offsets. HELIOS' predictions lie above CASMO's in the case of U-238 and below for Pu-239. In neither case, however, does the difference between the codes exceed 0.15 wt%. This is considered to be sufficient accuracy, given the preliminary nature of this study.

Table 2.5 Results of Isotopic Depletion Benchmark
(wt% based on total weight of all isotopes in table)

Isotope	HELIOS	CASMO	Difference	HELIOS	CASMO	Difference
	1 (GWd/MT) (wt%)			5 (GWd/MT) (wt%)		
U-235	3.795%	3.789%	0.006%	3.399%	3.371%	0.027%
U-238	96.167%	96.164%	0.003%	96.402%	96.383%	0.019%
Pu-238	0.000%	0.000%	0.000%	0.000%	0.000%	0.000%
Pu-239	0.037%	0.046%	-0.009%	0.183%	0.224%	-0.042%
Pu-240	0.001%	0.001%	0.000%	0.013%	0.017%	-0.004%
Pu-241	0.000%	0.000%	0.000%	0.003%	0.004%	-0.001%
Pu-242	0.000%	0.000%	0.000%	0.000%	0.000%	0.000%
Am-241	0.000%	0.000%	0.000%	0.000%	0.000%	0.000%
	16 (GWd/MT) (wt%)			36 (GWd/MT) (wt%)		
U-235	2.494%	2.433%	0.061%	1.325%	1.259%	0.066%
U-238	96.96%	96.901%	0.062%	97.720%	97.577%	0.143%
Pu-238	0.002%	0.003%	-0.001%	0.011%	0.019%	-0.008%
Pu-239	0.419%	0.508%	-0.089%	0.575%	0.691%	-0.115%
Pu-240	0.078%	0.098%	-0.021%	0.204%	0.242%	-0.038%
Pu-241	0.040%	0.051%	-0.011%	0.125%	0.163%	-0.038%
Pu-242	0.004%	0.005%	-0.001%	0.037%	0.046%	-0.009%
Am-241	0.000%	0.001%	0.000%	0.003%	0.004%	-0.001%

2.4 EMOX Model Description

A two-dimensional HELIOS model of a single standard Westinghouse 17X17 PWR assembly was developed for this EMOX performance survey. Model parameters are listed in Table 2.6 [P-1]. The model did not have a pellet to clad gap. Cladding material was homogeneously distributed across the area between the fuel pellet and the outer cladding boundary. Zircaloy-2 was used as a cladding material because Zircaloy-4 was not available in the HELIOS cross-section library. Control rod guide tubes were included in the model, though control rods themselves were not used in this study. Use of erbium in the model as a depletable neutron absorber will be discussed later.

Table 2.6 HELIOS Assembly Model Parameters

Parameter	Value
Fuel pellet radius (mm)	4.09575
Fuel cladding outer radius (mm)	4.7498
Fuel cladding material	Zircaloy-2
Fuel pin pitch (cm)	1.2598
Number of fuel rods per assembly	264
Guide thimble inner radius (mm)	5.6134
Guide thimble outer radius (mm)	6.0198
Guide thimble material	Zircaloy-2
Assembly pitch (cm)	21.5036
Active fuel height (ft)	12.0

Figures 2.3 and 2.4 present a detailed view of the HELIOS model. Figure 2.3 shows the spatial mesh which was employed within each fuel pin cell. The fuel area is divided into eight subregions and the moderator into five subregions in an effort to increase the accuracy of the depletion calculations. Mosteller performed sensitivity studies which compared HELIOS pin cell kinf results for various numbers of fuel region divisions to an MCNP pin cell calculation [M-2]. He found that the results were identical if eight separate fuel regions were used in the HELIOS model. Sensitivity studies of depletion calculations were not performed. Figure 2.4 displays the full assembly model. The positions of the fuel rods and the control rod guide tubes can easily be seen. The outer boundaries of the assembly are reflected such that an infinite core is simulated.

Figure 2.3 HELIOS Model of Westinghouse Pin Cell

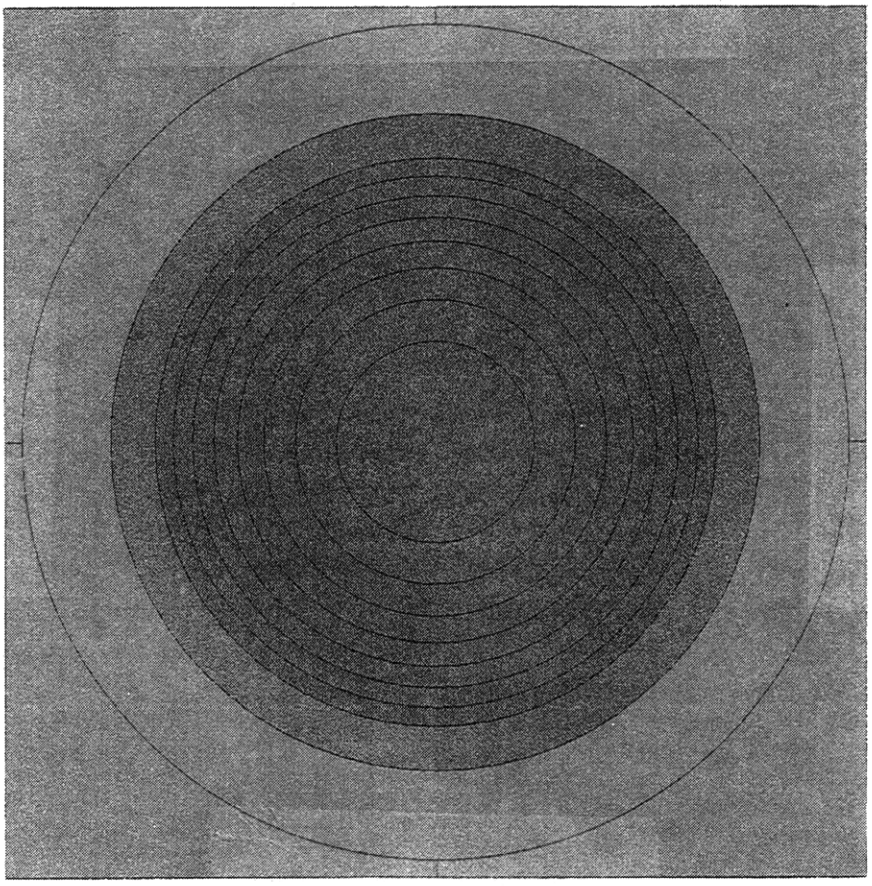

The eight darkest inner circles are the fuel regions. The next, slightly lighter circle represents the clad/gap, and the outermost five regions are moderator regions. The figure is drawn to scale. One inch on the page represents 0.28 cm.

Figure 2.4 HELIOS Model of Westinghouse 17 by 17 Assembly

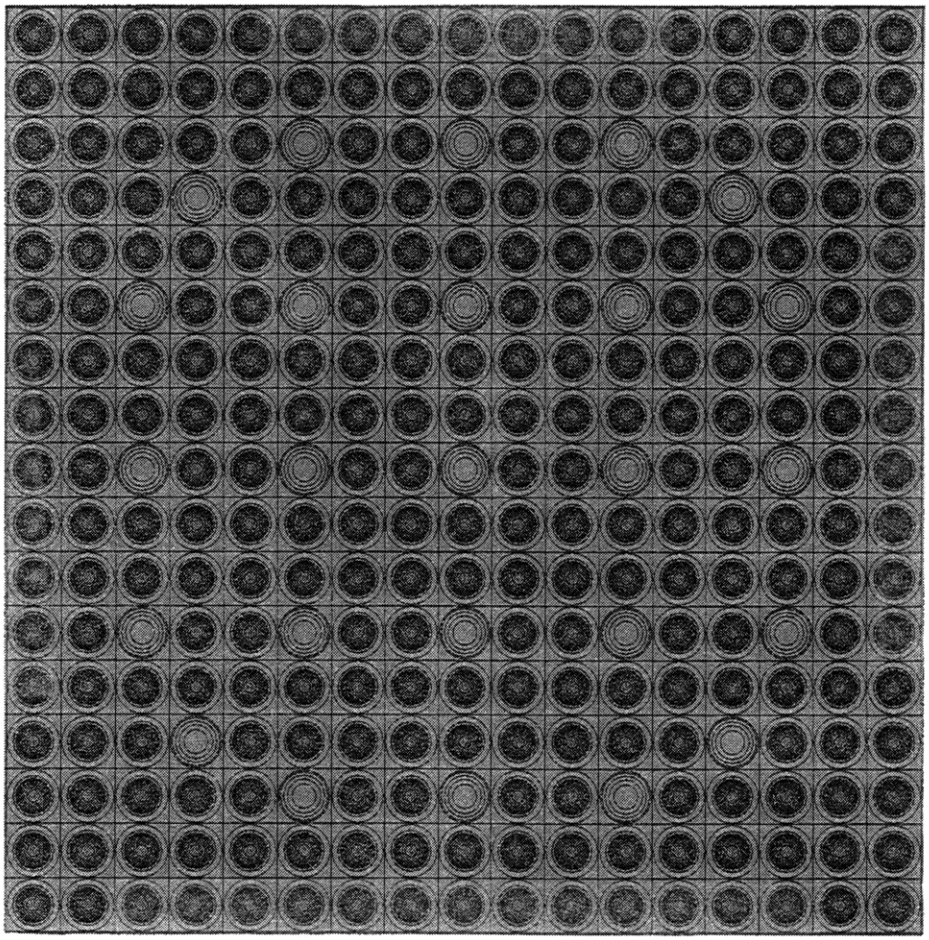

Squares containing dark inner circles are fuel pin cells. Squares containing lighter inner circles are coolant channels (empty control absorber channels). The figure is drawn to scale. One inch on the page represents 4.5 cm.

The assembly model was designed to simulate a full core of EMOX as it is burned through three 18-month equilibrium cycles. Different specific power levels were used during each cycle to simulate reducing assembly power levels consistent with current LWR fuel management. Each cycle was irradiated to a burnup equivalent to 439 days at each designated power level, which corresponds to 18 calendar months at a capacity factor of 80%. The burnup at the end of each cycle was determined according to the equations:

$$B_{cn}\ (\text{MWd/MT}) = P_n\ (\text{kW/kg}) \cdot 439.2\ (\text{days at power}) \qquad (2\text{-}1)$$

$$P_n\ (\text{kW/kg}) = [LHGR_{cn}\ (\text{kW/ft}) \cdot FH\ (\text{ft/pin})] / HM\ (\text{kg/pin}) \qquad (2\text{-}2)$$

where P_n is the specific power of cycle n for a given fuel composition, $LHGR_{cn}$ is the linear heat generation rate (LHGR) of cycle n, FH is the active fuel height and HM, is the mass of heavy metal per fuel pin.

Table 2.7 displays more of the assembly model parameters, including those which were varied from cycle to cycle. Power levels were assigned to be 110%, 100%, and 60% of the nominal average LHGR for a 4-loop PWR during the first, second, and third cycles, respectively [M-2]. This relative distribution of power between cycles was intended to simulate the typical power history of assemblies in three batch low leakage fuel management in which the assembly is moved to the core periphery during its third cycle. Consequently, a typical core at any given time would be comprised of one-third assemblies at cycle one power levels, one-third at cycle two power levels, and one-third at cycle three power levels. For the relative cycle power levels given above, the core average LHGR is only 90% of the nominal average for a 4-loop PWR because of the low power level of cycle three assemblies. The HELIOS model, then, corresponds to a core which is run at 90% of nominal average power for 16 months and then shut down for refueling during the

remaining two months of an 18-month fuel cycle. This gives the desired 80% overall capacity factor.

The soluble boron concentration in this model was, for the sake of simplicity, maintained constant at 750 ppm, which is about the average value over the course of a cycle. This approximation is not expected to appreciably affect the results of isotopic depletion calculations [M-2]. Fuel and cladding temperatures in the model also were not adjusted over the course of the fuel lifetime, but were kept at approximately average values. Fuel temperatures were varied across the concentric model regions, ranging from 1200 K for the innermost circular fuel region down to 750 K at the fuel's outer edge. Moderator temperatures were adjusted to mirror power level change at the beginning of each cycle. Corresponding density changes were then computed and used to adjust the input number densities of the moderator's constituents (hydrogen, oxygen, and most notably, natural boron). One sample of the HELIOS input generated for this model can be found in Appendix C. The exact geometry used in all HELIOS assembly calculations can be inferred from this input.

Table 2.7 Assembly Model Parameters by Cycle

Parameter		Value		
Nominal average LHGR (kW/ft) for a 4-loop PWR		5.58		
Weighted (as used) $LHGR_{cn}$ (kW/ft):	Cycle 1	6.138		
	Cycle 2	5.58		
	Cycle 3	3.348		
Average of weighted $LHGR_{cn}$ (kW/ft) values		5.022		
Implied average power during operation		90% (of nominal value)		
Moderator soluble boron concentration (ppm)		750		
Fuel temperatures (K)		750-1200		
Fuel cladding temperature (K)		650		
Moderator temperature (K):	Cycle 1	605.37		
	Cycle 2	582.04		
	Cycle 3	572.04		
Refueling shutdown period during each cycle		2 months		
Overall core capacity factor		80%		
Number Densities (atoms/barn-cm):		Cycle 1	Cycle 2	Cycle 3
	Zircaloy-2 (cladding)	3.7376×10^{-2}	same	same
	B-10 (in coolant)	5.3542×10^{-6}	5.8808×10^{-6}	6.0607×10^{-6}
	B-11 (in coolant)	2.1552×10^{-5}	2.3671×10^{-5}	2.4395×10^{-5}
	H-1 (coolant)	4.3093×10^{-2}	4.7331×10^{-2}	4.8779×10^{-2}
	O-16 (coolant)	2.1547×10^{-2}	2.3665×10^{-2}	2.4390×10^{-2}

The fuel material itself was, as previously described, composed of varying amounts of PuO_2, UO_2, ZrO_2-CaO, and Er_2O_3. The ratio of CaO to ZrO_2 was constant at 15 vol.%. This CaO presence is intended to stabilize the fluorite phase of the ZrO_2. The HELIOS library contains identifiers for natural zirconium and calcium, and these were used in the EMOX fuel model. Uranium and erbium were modeled via individual isotopes which were

weighted so as to approximate the natural abundances of the elements . There are two naturally occurring isotopes of erbium, Er-162 and 164, which are not contained in HELIOS' library, however. These isotopes compose less than two percent of natural erbium and their combined macroscopic thermal absorption cross section represents 0.15 percent of the macroscopic cross section for all erbium isotopes. The absence of Er-162 and 164, therefore, is unlikely to have a significant effect on the calculations described here. The missing isotopes were represented in the HELIOS model by additional Er-166. Finally, the RGP in the model was represented by Pu-238 through 242. The isotopic percentages used for plutonium, uranium, and erbium can be found in Table 2.8.

Table 2.8 Isotopic Composition of Fuel Materials

Element	Isotope	Atom Percent
Uranium	235	0.7%
	238	99.3%
Plutonium	238	1.15%
	239	59.81%
	240	20.14%
	241	14.53%
	242	4.37%
Erbium	166	7.07%
	167	4.59%
	168	5.36%
	170	2.98%

The fuel components were distributed homogeneously throughout each fuel pin, and all fuel pins in an assembly were identical. The homogeneous distribution of erbium bears some discussion. Some depletable neutron absorbers, e.g. gadolinium, are often used in only a small fraction of the fuel pins in each assembly. Gadolinium has a very large neutron capture cross section and would tend to deplete very quickly if used in the

small quantities that would be required in each fuel pin in the case of homogeneous distribution. If it is employed in much higher concentrations in a smaller number of fuel pins, the gadolinium is self-shielded such that it depletes in layers from the outside of the fuel pin towards the center. The gadolinium can thus act as an absorber for a much longer portion of the cycle.

Erbium has a much smaller capture cross section than gadolinium and, because of its isotopic composition, tends to be somewhat self-regenerating. Erbium contains a single isotope, Er-167, which is a significant thermal and epithermal absorber [A-1]. However, when Er-166 (which comprises 33.6% of natural erbium) undergoes a neutron capture it becomes Er-167 and thus is likely to undergo yet another capture. This behavior coupled with its relatively small capture cross section allows erbium to perform as a long-lasting depletable neutron absorber even in small concentrations.

Unfortunately, some fraction of the erbium which is incorporated into fresh fuel will remain even at the end of the fuel lifetime. This residual reactivity hold down must then be accommodated via an increased overall fissile enrichment in the fuel. Many depletable neutron absorbers suffer from this drawback. However, erbium residuals are somewhat higher than those for gadolinium, for instance. The penalty for the addition of 1.0 vol.% erbia to the 3 vol.% PuO_2, 30 NFP EMOX composition in this work, for example, is about a 0.02 difference in the EOC core average reactivity. This disadvantage can be minimized if the erbium is distributed relatively homogeneously throughout the fuel [A-1]. In addition, homogeneously distributed erbium can minimize power peaking over the course of a fuel cycle [J-1]. For the purposes of this study, therefore, the advantages of homogeneously distributed erbium are believed to outweigh those of alternative absorber loading strategies [A-1, M-1].

2.5 UO_2 Comparison Calculation

The model described in Section 2.4 was also used to burn a uranium fueled assembly. This calculation was done in order to establish a performance baseline with which to compare the various EMOX compositions. The uranium assembly pin compositions were designed by Yankee Atomic Electric Company in Bolton, Massachusetts for use in a Westinghouse 4-loop PWR with an 18-month fuel cycle [Y-1]. This design also makes use of erbium as a depletable neutron absorber. Unlike the EMOX assemblies, however, the erbium is used in only a fraction of the uranium fuel pins. Figure 2.9 shows the location of the erbium-containing fuel pins in the uranium fuel design. All of the fuel pins in this assembly use 4.4% enriched UO_2. The erbium pins also contain 1.2 wt% Er_2O_3. All model parameters not pertaining to fuel composition were identical to those used for examining EMOX compositions.

2.6 CASMO-3 Comparison Calculations

CASMO-3 is a two-dimensional transport theory code designed to perform burnup calculations on BWR and PWR pin cells and assemblies [E-1]. The code has a 70-group neutron data library which is based on ENDF/B-IV. CASMO is widely used in the nuclear power industry. A few of the EMOX assembly calculations described in section 2.4 were duplicated using CASMO-3 in order to confirm results given by HELIOS. The assembly model parameters in the CASMO-3 calculations were identical to those used in HELIOS whenever possible. A small number of modifications were necessary to accommodate the differences between the libraries and input formats of the two codes.

All of the dimensions in the CASMO model were identical to those in the HELIOS model. Materials substitutions were necessary, however, in that CASMO's library does not contain natural zirconium or calcium. The library does contain a single material identifier which represents Zircaloy-2 and 4. This material was used in place of the

Figure 2.5 HELIOS Model of Westinghouse UO_2 Fueled Assembly

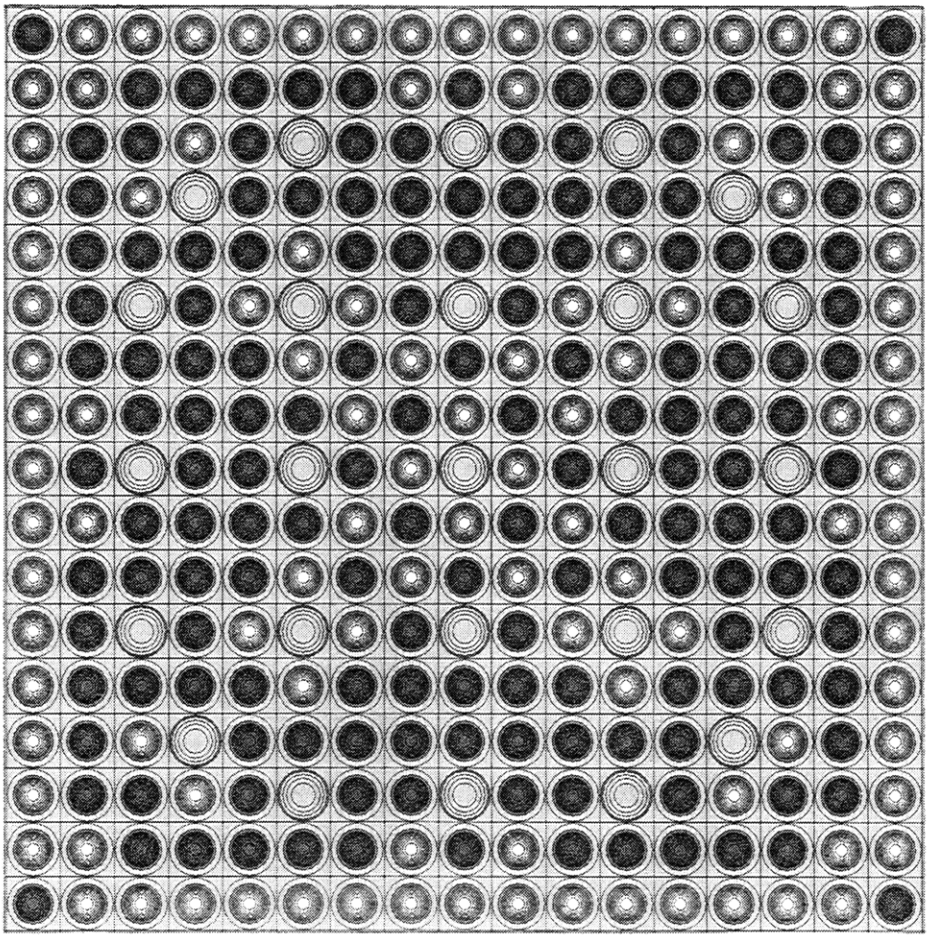

Squares containing small, white inner circles are uranium (4.4% enriched) fuel pin cells. Squares containing dark inner circles are uranium pins which also contain 1.2 wt% Er_2O_3. Squares with larger, lighter inner circles are coolant channels (empty control absorber channels.) The figure is drawn to scale. One inch on the page represents 4.5 cm.

zirconium in EMOX fuel, and aluminum was substituted for calcium. These substitutions are thought to have negligible impact on simulation results because these materials all have very small neutron cross sections. Initial fuel compositions in the two codes were identical save that HELIOS requires material number densities as input while CASMO uses weight percentages and material densities. The EMOX fuel densities used in CASMO were calculated via volume weighted averages of the densities of individual EMOX components.

CASMO, unlike HELIOS, assigns a single temperature to the fuel region. The average of the various fuel region temperatures used in HELIOS (1037 K) was, therefore, assigned to the fuel in CASMO. The assembly moderator temperature was changed at the beginning of each cycle during the CASMO runs as it was in HELIOS. CASMO automatically adjusts the moderator density to correspond with changes in temperature while in HELIOS, the moderator number density during each cycle was specified in the input. The fuel was depleted to the same burnup during each cycle in both codes. The exact burnup steps were specified in HELIOS, however, while CASMO's default depletion steps were used. An example of the CASMO input used for these calculations is found in Appendix C.

2.7 Summary

A model of a typical 4-loop Westinghouse PWR assembly is used in this study to evaluate the performance of various EMOX compositions through a simulation of three 18-month equilibrium cycles. A different power level is used during each of the cycles to simulate the experience of an assembly as it is placed in different core locations. A capacity factor of 0.8 is taken into account in calculating cycle burnup values, and the moderator boron concentration is held at a constant 750 ppm throughout each assembly's lifetime. The same model is also used to simulate a standard Westinghouse uranium fueled assembly, but with erbium as a depletable neutron absorber, for comparison with EMOX results.

EMOX depletion and criticality calculations are performed using the HELIOS code developed by Scandpower. HELIOS is a two-dimensional collision probability code capable of supporting general geometries. The code has been benchmarked for accuracy in both criticality and isotopic depletion calculations. A small number of EMOX cases were also run using the CASMO-3 code as an additional verification of HELIOS EMOX results.

CHAPTER THREE: RESULTS

3.1 Introduction

This chapter reviews the results of the reactivity and burnup calculations. First, a brief overview of the reactivity behavior of various EMOX compositions as a function of burnup is given. Next, fuel assembly calculations comparing the average BOC and EOC core reactivities for each composition are presented. Criteria are then suggested for using these values to select the most promising cases for further study. The second section of this chapter examines the plutonium destruction capabilities of the recommended compositions, including an analysis of the changes in particular plutonium isotopes. Finally, comparisons between CASMO-3 and HELIOS results are made.

3.2 Analysis of EMOX Reactivity Behavior

3.2.1 Examples of EMOX Reactivity Behavior as a Function of Burnup. Many different EMOX compositions were examined in this work. In this section, the reactivity versus burnup behavior of some of the extreme compositions is discussed in order to give a feeling for the overall results of the study. For the sake of convenience, reactivity (ρ or

rho) is used instead of the k_{inf} values due to its near-linear relationship with burnup. The burnup of the fuels is quoted in terms of MWd/m^3. The conversion from the conventional MWd/MT to MWd/m^3 is made by multiplying the former by the mass of heavy metal per unit volume in a given fuel composition. This unconventional unit is necessary to make direct comparisons between EMOX and UO_2 compositions, which have drastically different heavy metal loadings.

Figure 3.1 shows the ρ behavior of EMOX compositions containing 6 vol.% PuO_2, no Er_2O_3, and a variety of non-fertile loadings. A pure MOX case is included for comparison. Transitions between cycles are clearly marked by discontinuities in ρ. These artifacts are caused by instantaneous decreases in power level and equilibrium xenon and samarium levels. It is interesting to note that at this particular plutonium loading, the compositions with the highest reactivity during the first and second cycle are those with the lowest fertile loadings. Recall that a higher non-fertile loading means a correspondingly lower loading of natural uranium. The lower U-238 content leads to a reduction in parasitic absorptions which more than compensates for the reactivity loss due to lower U-235 content. The result is an increase in ρ at the BOC. During the third cycle, however, the additional Pu-239 production results in higher reactivity among the compositions with a higher U-238 content. In general then, higher reactivity at zero burnup corresponds to a steeper slope of reactivity vs. burnup--a self compensating effect since reactivity limited burnup capability depends on the ratio of $\rho(0)$ to $d\rho/dB$ in the linear reactivity model of core behavior [D-1]. The effects of these competing processes on the overall core reactivity are discussed in more detail later in this chapter.

Figure 3.1 Reactivity vs. Burnup Behavior of EMOX/MOX Cases with 6 vol.% PuO_2, 0 vol.% Er_2O_3

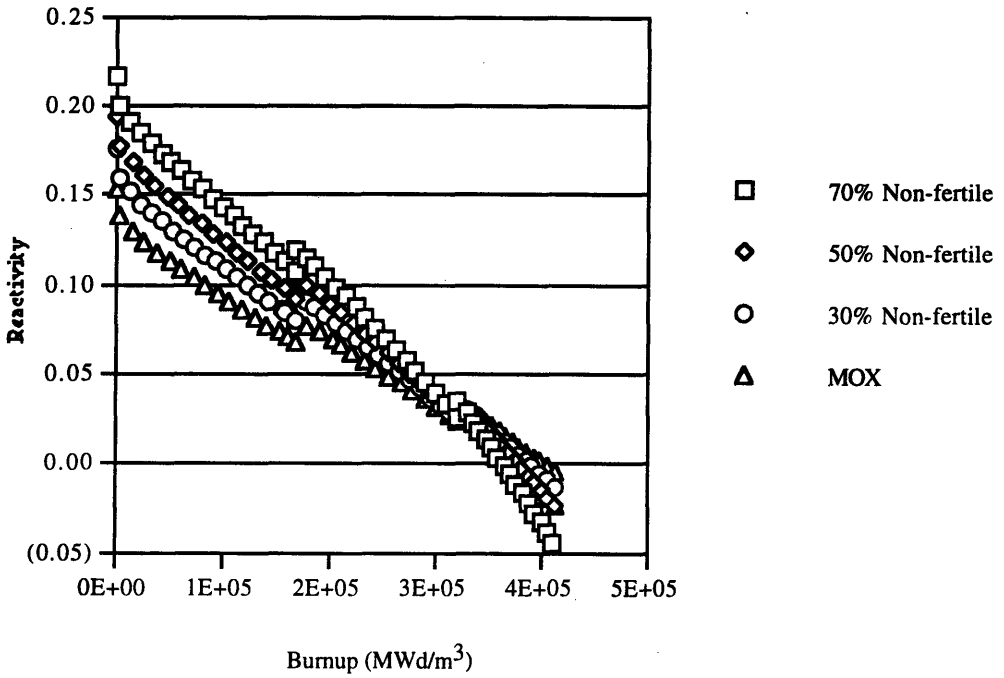

Note: Data plotted in the Figures of this thesis can be obtained from Prof. M. J. Driscoll of the MIT Nuclear Engineering Department.

Figure 3.2 presents ρ behavior for EMOX compositions of 6 vol.% PuO_2, 70 vol.% ZrO_2-CaO, and Er_2O_3 loadings ranging from 0.0-1.5 vol.%. Lower erbia loadings result in higher reactivities throughout all three cycles, as would be expected. In each case, about 70% of the Er-167 is burned by the end of the first cycle. Some Er-167 remains, however, even at the end of the second (about 9%) and third (about 5%) cycles. The residual erbium, and its associated reactivity penalty, have a substantial impact on the reactivity balance of the overall core. The magnitude of this impact is examined in Section 3.2.2.

Figure 3.2 Reactivity vs. Burnup Behavior of EMOX Cases with 6 vol.% PuO_2, 70 vol.% Non-Fertile Material

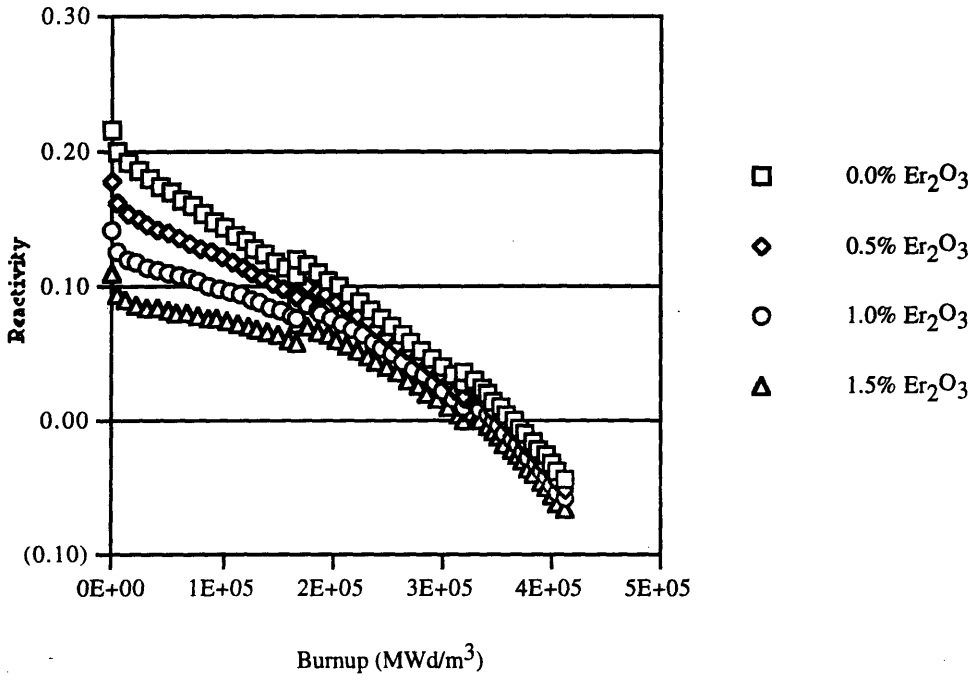

Figure 3.3 shows EMOX cases containing 1.5 vol.% Er_2O_3, 70 vol.% ZrO_2-CaO, and 3-6 vol.% PuO_2. The curves have similar slopes during the first fuel cycle, but are offset by a small amount due to their different fissile loadings. This difference becomes distinctly more pronounced, however, as the cases with lower fissile loadings begin to burn out during the second and third cycles. This effect is especially severe because these compositions contain little (less than 30 vol.%) fertile U-238 and so are less able to compensate for the loss of initial fissile material through Pu-239 breeding.

Figure 3.3 Reactivity vs. Burnup Behavior of EMOX Cases with 1.5 vol.% Er_2O_3, 70 vol.% Non-Fertile Material

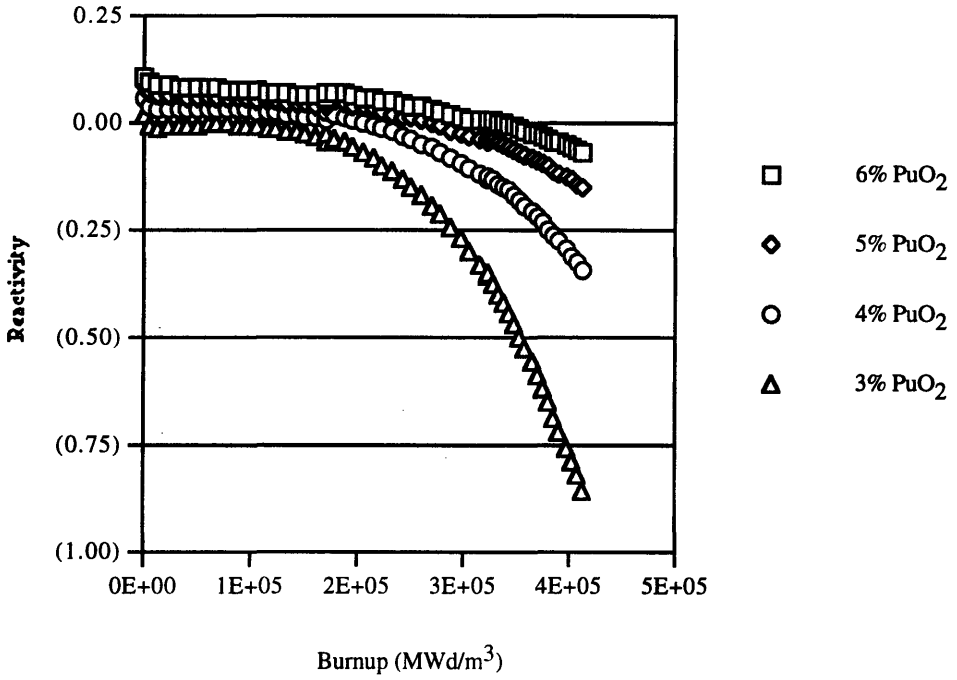

3.2.2 Evaluation of Core-Average Reactivity Values. An EOC core-average reactivity (ρ_{core}) value was calculated for each EMOX composition to be used as a gauge of whether a particular composition can remain critical during the simulated cycle of 18 calendar months. Core average reactivity values are calculated for the case of a PWR equilibrium core containing one-third fresh EMOX assemblies, one-third once-burned EMOX assemblies, and one-third twice-burned EMOX assemblies. Thus, the reactivity value at the end of each cycle of a given EMOX assembly simulation represents the reactivity contribution to a whole core containing one-third assemblies of this category. Now, recall that each cycle of the assembly simulations was run at a different specific power. In averaging the contributions of each cycle or set of assemblies, the relevant fraction of the total core power can be used to weight the various reactivity values to obtain a more accurate result than

simple equal power sharing (i.e. simple number weighting) [D-1]. The equations for ρ_{core} take the following form:

$$\rho_{core} = f_1\rho_1 + f_2\rho_2 + f_3\rho_3 \qquad (3\text{-}1)$$

$$\text{where} \quad f_n = (\text{ LHGR of cycle n }) / (\ \Sigma \text{ LHGR of cycle n }) \qquad (3\text{-}2)$$

$$\text{and} \quad \rho_n = \text{EOC reactivity value for cycle n.}$$

The calculated EOC values of ρ_{core} for all EMOX compositions can be found in Table 3.1. The EOC core average reactivity values for MOX cases, which contain no erbia or non-fertile material, and the uranium fuel composition discussed in Chapter 2 are listed in Table 3.2.

Table 3.1 Excess Core Averaged Reactivity at EOC for EMOX Compositions

30% Non-Fertile EMOX

	Volume Percent Er_2O_3 in EMOX Fuel			
Vol.% PuO_2	0.0%	0.5%	1.0%	1.5%
3.0%	-0.07870	-0.08826	-0.09814	-0.10839
4.0%	-0.02247	-0.03151	-0.04327	-0.05426
5.0%	0.01365	0.00296	-0.00815	-0.01966
6.0%	0.03946	0.02846	0.01710	0.00531

50% Non-Fertile EMOX

	Volume Percent Er_2O_3 in EMOX Fuel			
Vol.% PuO_2	0.0%	0.5%	1.0%	1.5%
3.0%	-0.12642	-0.13683	-0.14761	-0.15871
4.0%	-0.03820	-0.04875	-0.05969	-0.07101
5.0%	0.01058	-0.00030	-0.01158	-0.02330
6.0%	0.04205	0.03091	0.01934	0.00743

70% Non-Fertile EMOX

	Volume Percent Er_2O_3 in EMOX Fuel			
Vol.% PuO_2	0.0%	0.5%	1.0%	1.5%
3.0%	-0.28777	-0.30392	-0.32060	-0.33793
4.0%	-0.08422	-0.09626	-0.10876	-0.12169
5.0%	-0.00008	-0.01146	-0.02326	-0.03547
6.0%	0.04349	0.03211	0.02035	0.00822

Note: Shaded entries were deemed acceptable based on EOC reactivity criteria.

Table 3.2 Excess Core Averaged Reactivity at EOC for MOX and UO_2 Compositions

	MOX	UO_2
Vol.% PuO_2	ρ_{core}	ρ_{core}
3.0%	-0.05096	-0.04499
4.0%	-0.01317	
5.0%	0.01422	
6.0%	0.03564	

Note: Shaded entries were deemed acceptable based on EOC reactivity criteria.

Several expected trends can be seen in the EOC ρ_{core} values. Increased fuel plutonium loadings result in higher core reactivities, while increased erbia loadings diminish core reactivities. The changes in ρ_{core} as a function of non-fertile percentage (NFP), however, are more complex. At low plutonium loadings (5 vol.% PuO_2 or less) EOC core reactivity decreases with increasing non-fertile loading, as can be seen in Figure 3.4. This trend becomes less exaggerated with increasing PuO_2 loadings, however, until at 6 vol.% PuO_2 there is a slight increase in EOC ρ_{core} values with increasing NFP. The reason for this change can be traced to the reactivity vs. burnup behavior of EMOX compositions with varying NFPs (as shown for 6 vol.% PuO_2 cases in Figure 3.1). Compositions with higher NFPs have higher reactivities during the first and much of the second fuel cycle due to a decrease in parasitic neutron absorption by U-238. The first and second cycles are run at higher power levels and, therefore, have a greater influence on the power weighted core averaged reactivity. Higher plutonium loadings also result in higher assembly reactivities, particularly at EOL (see Figure 3.3). Thus, the increase in BOL reactivity which accompanies higher NFPs coupled with the increase in EOL reactivity derived from additional plutonium results in increasing EOC core average reactivity values as a function of NFP for 6 vol.% PuO_2 EMOX compositions. Figure 3.4 shows ρ_{core}

values for EMOX cases containing 1.5 vol.% erbia, but the trends shown in the graph hold for all of the erbia loadings which were investigated.

Figure 3.4 Excess Core Averaged Reactivity at EOC vs. Fuel Non-Fertile Loading for EMOX Cases with 1.5 vol.% Er_2O_3

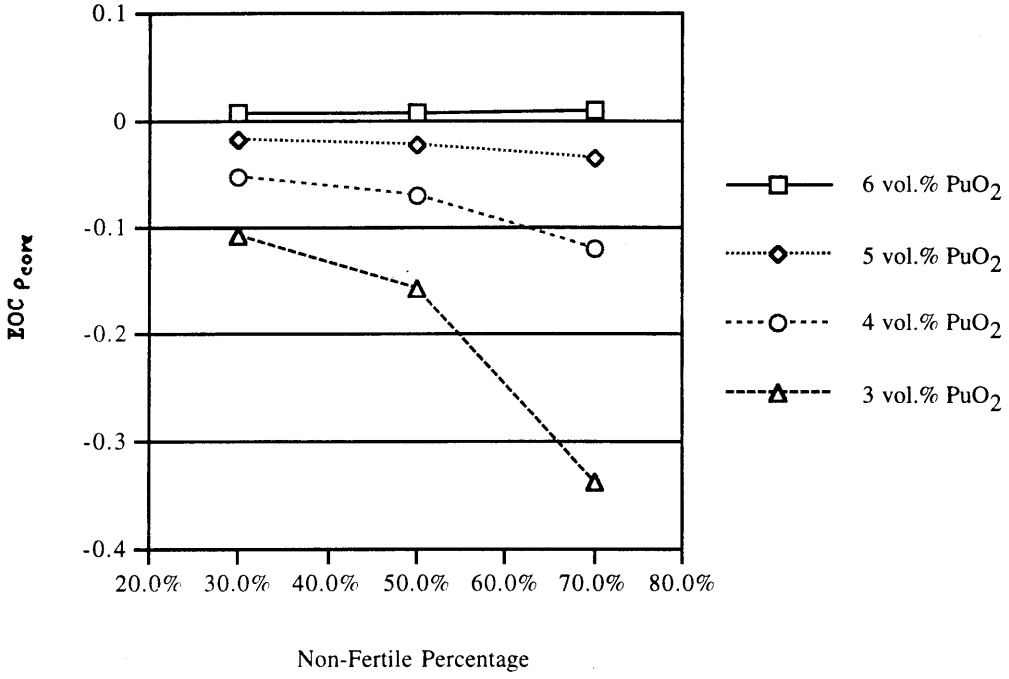

All of the assemblies were modeled as effectively infinite systems and were run with a constant 750 ppm natural boron in the light water coolant. Ideally, we would like to calculate the excess reactivity available in a finite core fueled with a given EMOX composition in the absence of soluble boron. The ρ_{core} values calculated above are, therefore, somewhat biased as they do not include the effects of neutron leakage on a finite core, nor compensate for the impact of the boron. Neutron leakage reduces the excess core reactivity while the removal of 750 ppm soluble boron increases ρ_{core}. The magnitude of these effects would vary slightly depending on the particular fuel composition due to subtle neutron spectrum effects associated with how one strikes a neutron balance in assembly calculations (see Chapter 6 of reference D-1). For the purposes of this work, the effects of

750 ppm soluble boron and neutron leakage will be assumed to be approximately the same for all compositions and therefore not have a significant impact on observed trends. More accurate calculations would require a whole core simulation with ρ kept at zero by varying soluble boron.

The average neutron leakage of a PWR core under low-leakage fuel management is approximately 2.5% [B-2]. This corresponds to approximately 1.5% radial leakage and 1.0% axial leakage. The effect of the soluble boron on ρ_{core} is determined here by running EMOX cases with no boron and comparing their core reactivity values to those of the original 750 ppm boron cases. This was done for two example cases using CASMO-3. The results appear in Table 3.3.

Table 3.3 EOC Excess Core Averaged Reactivity Values for EMOX Cases with and without Soluble Boron

EMOX Composition (by vol.%)	ρ_{core} (with boron)	ρ_{core} (without boron)	$\Delta\rho_{core}$
6% PuO_2, 1.5% Er_2O_3, 50% ZrO_2-CaO	-0.00734	0.01940	0.02674
6% PuO_2, 1.5% Er_2O_3, 70% ZrO_2-CaO	-0.00779	0.02338	0.03117

Thus, for the cores examined in this work, the reactivity loss due to neutron leakage is assumed to be approximately equal to the reactivity loss which accompanies the presence of 750 ppm of natural boron. In other words, the effects of leakage and of soluble boron can be ignored in analyzing the original ρ_{core} values because these effects cancel one another out.

In Tables 3.1 and 3.2, positive ρ_{core} values indicate that at the end of an 18 month cycle a given composition contains enough fissile material to continue to burn, while

negative values correspond to cores which are not capable of remaining critical for the full cycle length. The EOC ρ_{core} values, then, should be approximately zero in the ideal case of maximum possible fuel utilization. Notice, however, that the nominal 18 month equilibrium cycle uranium assembly which was run as a comparison resulted in a negative ρ_{core} value. The HELIOS model used in this study is only an approximate representation of the processes involved in burning a full equilibrium PWR core through an 18 calendar month cycle, and as such does not give precise results. For the purposes of this work, therefore, we assume that the ρ_{core} value of the uranium case does represent a viable fuel. Accordingly, only cases with ρ_{core} values less than -0.05 are considered inherently unable to remain critical for the duration of the cycle. The compositions which are found to be able to support 18 month cycles are listed in Table 3.4.

Table 3.4 EMOX Compositions Deemed Capable of Supporting an 18-month Cycle

PuO_2 Vol.%	Er_2O_3 Vol.%
30% Non-fertile	
4.0	0.0-1.0
5.0	0.0-1.5
6.0	0.0-1.5
50% Non-fertile	
4.0	0.0-0.5
5.0	0.0-1.5
6.0	0.0-1.5
70% Non-fertile	
5.0	0.0-1.5
6.0	0.0-1.5

Not all of the remaining compositions are necessarily acceptable from the standpoint of other neutronic and safety considerations. The acceptability of reactivity coefficients of these compositions is left to future work. Next, we discuss only the impact of the maximum allowable soluble boron concentration which corresponds to water chemistry constraints .

In practice, soluble boron is dispersed in the water moderator of a PWR in such a way that the overall reactivity of the core is always kept at zero. Thus, at earlier points in a given cycle, more boron is required because the overall core excess reactivity will be higher. High soluble boron concentrations can contribute to corrosion of the structural materials in a reactor core [M-1, H-1]. In order to limit this, a maximum allowable boron concentration is set. This maximum will depend on various factors such as the coolant temperature, pH, and lithium concentration. In a Westinghouse PWR, this value is roughly 2,000 ppm [M-3].

The maximum core average excess reactivity for all of the cases modeled in this work is found at the beginning of the fuel cycle (BOC). The value of this BOC core reactivity can be computed in a manner analogous to that used to find the EOC ρ_{core}. This BOC ρ_{core} is computed for the sample cases mentioned above that were run both with and without 750 ppm soluble boron. The results are found in Table 3.5. An approximate core boron coefficient can then be found by dividing the BOC $\Delta\rho_{core}$ by 750 ppm. For the purposes of this work, an approximate boron coefficient of 3.0×10^{-5} $\Delta\rho$/ppm is adopted. Finally, given the maximum allowable boron concentration, a maximum BOC ρ_{core} of 0.06 is obtained. This represents an estimate of the highest BOC average core reactivity which will be controllable with soluble boron while respecting coolant chemistry control limits.

Table 3.5 BOC Excess Core Averaged Reactivity Values for EMOX Cases with and without Soluble Boron

EMOX Composition (by vol.%)	ρ_{core} (with boron)	ρ_{core} (without boron)	$\Delta\rho_{core}$	Boron Coefficient ($\Delta\rho$/ppm)
6% PuO_2, 1.5% Er_2O_3, 50% ZrO_2-CaO	0.04668	0.06909	0.02241	2.988×10^{-5}
6% PuO_2, 1.5% Er_2O_3, 70% ZrO_2-CaO	0.05965	0.08387	0.02422	3.229×10^{-5}

Table 3.6 presents the BOC excess core reactivity values for those EMOX cases which were deemed reactive enough to sustain at least the nominal 18 month cycle. Those compositions whose BOC ρ_{core} values are lower than the 0.06 limit are highlighted. The same is true for the BOC ρ_{core} values of the MOX and UO_2 compositions which are found in Table 3.7. Recall that the MOX compositions contained no erbia. It is not surprising, therefore, that they are all too reactive at the beginning of the fuel cycle. Table 3.8 lists all of the EMOX compositions which satisfy both the BOC and EOC reactivity criteria.

It should be noted that cores exceeding 0.06 might be made suitable using other burnable neutron absorbers, such as gadolinium or europium, to hold down BOC excess reactivity. Various authors have studied innovative neutron absorber loadings for UO_2, MOX, and non-fertile fuel compositions [C-1, P-2, A-1, D-2].

Table 3.6 Excess Core Averaged Reactivity at BOC for EMOX Compositions

30% Non-Fertile EMOX				
	Volume Percent Er_2O_3 in EMOX Fuel			
Vol.% PuO_2	0.0%	0.5%	1.0%	1.5%
4.0%	0.07523	0.04834	0.02147	
5.0%	0.09703	0.07167	0.04792	0.02536
6.0%	0.11373	0.09032	0.06844	0.04752
50% Non-Fertile EMOX				
	Volume Percent Er_2O_3 in EMOX Fuel			
Vol.% PuO_2	0.0%	0.5%	1.0%	1.5%
4.0%	0.08137	0.05324		
5.0%	0.10690	0.08131	0.05733	0.03452
6.0%	0.12515	0.10157	0.07943	0.05836
70% Non-Fertile EMOX				
	Volume Percent Er_2O_3 in EMOX Fuel			
Vol.% PuO_2	0.0%	0.5%	1.0%	1.5%
5.0%	0.11838	0.09262	0.06849	0.04553
6.0%	0.13965	0.11600	0.09378	0.07258

Note: Shaded entries were deemed acceptable based on BOC and EOC reactivity criteria.

Table 3.7 Excess Core Averaged Reactivity at BOC for MOX and UO_2 Compositions

MOX		UO_2
Vol.% PuO_2	ρ_{core}	ρ_{core}
4.0%	0.06560	0.05509
5.0%	0.08457	
6.0%	0.10004	

Note: Shaded entries were deemed acceptable based on BOC and EOC reactivity criteria.

Table 3.8 EMOX Compositions Meeting BOC and EOC Reactivity Criteria

PuO_2 Vol.%	Er_2O_3 Vol.%
30% Non-fertile	
4.0	0.5
	1.0
5.0	1.0
	1.5
6.0	1.5
50% Non-fertile	
4.0	0.5
5.0	1.0
	1.5
6.0	1.5
70% Non-fertile	
5.0	1.5

The 5.0% PuO_2, 1.5% Er_2O_3 EMOX compositions, all of which were selected based on the BOC and EOC criteria, are shown in Figure 3.5 along with the UO_2 case. These EMOX cases have smaller reactivity swings than the uranium case. This is probably because the UO_2 composition has been optimized to maximize the amount of energy which

can be extracted from the fuel, whereas no attempt has been made to optimize the EMOX compositions studied here. These cases demonstrate, however, that EMOX can be designed to have a smaller lifetime reactivity swing than UO_2 fuel. With the exception of some of the latter half of the 70% NFP curve, the EMOX curves also maintain smaller slopes than the uranium curve. The reactivity behavior of the other chosen EMOX compositions will be similar to that shown in Figure 3.5, with small adjustments according to the trends noted in the beginning of this chapter. In general, then, the chosen EMOX cases compare well with the reference uranium case in terms of reactivity behavior.

Figure 3.5 Reactivity vs. Burnup Behavior of EMOX Cases with 5 vol.% PuO_2, 1.5 vol.% Er_2O_3 and UO_2 with Er_2O_3

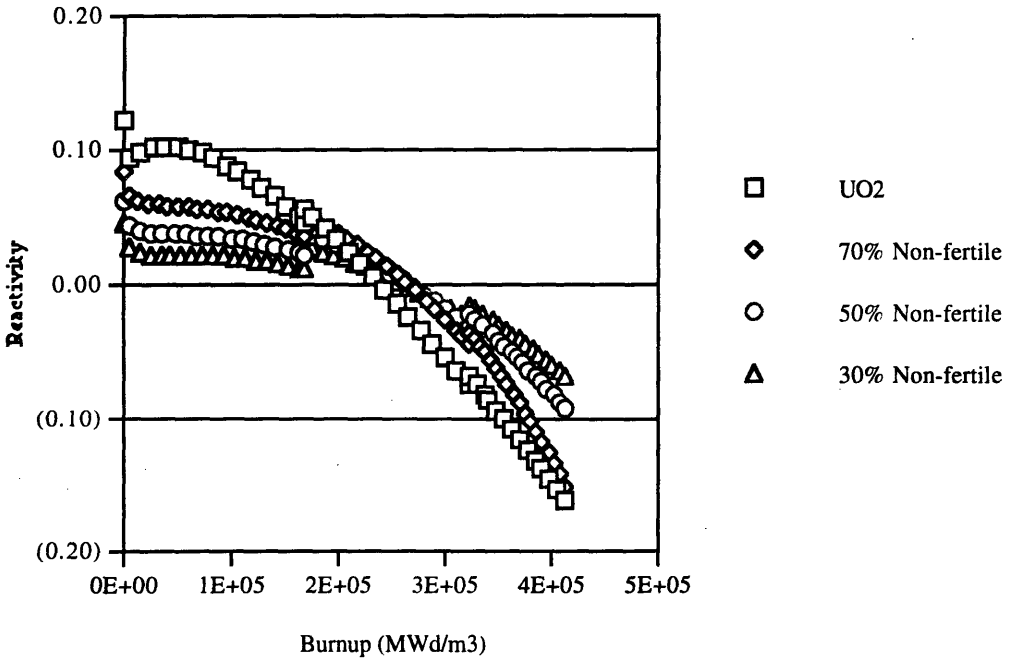

A few final notes should be made regarding the chosen EMOX compositions. The impact of additional erbia on the EMOX EOC core reactivities can be seen in Table 3.1. Incrementing the erbia loading by 0.5 vol.% changes the EOC ρ_{core} by about 0.01, though this figure increases slightly (up to approximately 0.012) for cases with higher NFPs and PuO_2 loadings. All of the EMOX compositions in this study have been given in volume

percentages of constituent compounds rather than the more standard industry wt% designations. The correspondence between the PuO_2 loading in a given EMOX composition by volume percent and the same PuO_2 loading in MOX by weight percent is given in Table 3.9. Note that fuels with identical PuO_2 loadings will have identical plutonium metal loadings as well. The PuO_2 volume and weight percents are roughly the same over the range of loadings we are interested in. The difference in volume and weight percent is greater at higher loadings.

Table 3.9 Total PuO_2 Loading by Weight and Volume Percent

Volume Percent in EMOX or MOX (independent of NFP)	Total Pu Number Densities (atoms/barn-cm)	Weight Percent in MOX (natural uranium)
4.0%	1.0163×10^{-3}	4.18%
5.0%	1.2704×10^{-3}	5.22%
6.0%	1.5245×10^{-3}	6.26%

Note: Multiply total PuO_2 loading by 0.7434 to get fissile PuO_2 loading.

3.2.3 Comparison of HELIOS and CASMO-3 Calculated Reactivity Values for Selected Cases. A select number of EMOX cases were run using CASMO-3 as an additional check on the results of the HELIOS simulations. Graphical comparisons of these results are found in Figures 3.6 and 3.7. The figures show that at the beginning of the first cycle, the codes agree almost exactly. The difference between the two results, however, grows with increasing burnup. After three 18 month cycles, the predicted ρ values are off by approximately 0.03. The EOC core average reactivity values derived from the two codes are slightly closer because of the heavier weighting on the early cycles. There are many possible causes of the discrepancies between the codes. Resonance capture treatments in U-238 and Pu-240 could differ, for example. Table 3.10 shows the EOL plutonium isotopics for a single EMOX case (6 vol.% PuO_2, 1.5 vol.% Er_2O_3, NFP 70) as computed

Figure 3.6 Comparison of CASMO/HELIOS Reactivity Results for EMOX with 6 vol.% PuO_2, 1.5 vol.% Er_2O_3, and 50 vol.% Non-fertile Material

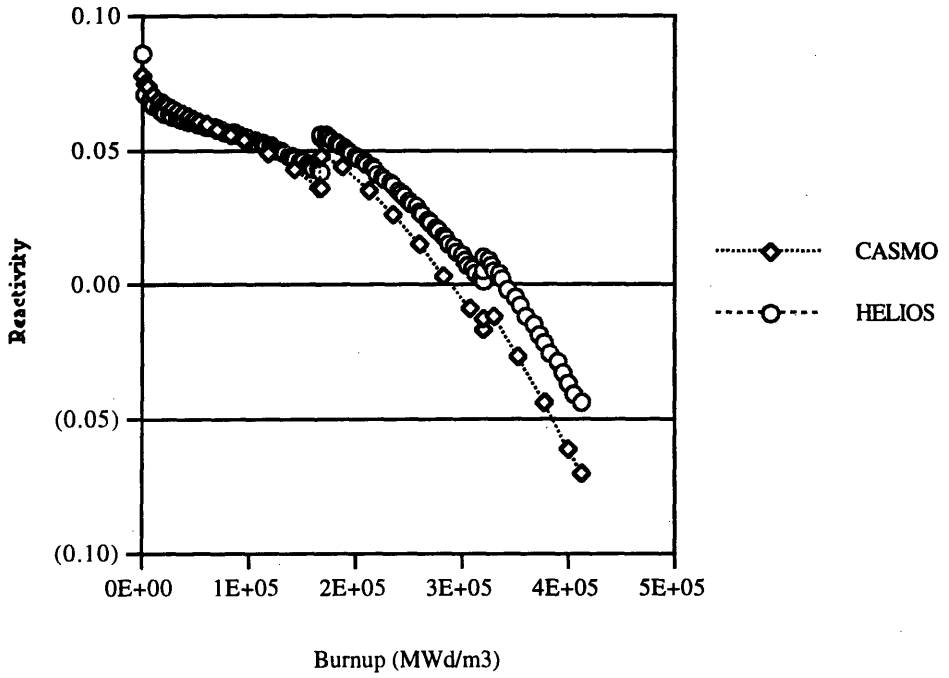

by HELIOS and CASMO-3. The differences between these results would seem to indicate some differences in the way the two codes handle these isotopes. Discrepancies between HELIOS and CASMO were not investigated any further as part of this work, however. For the purposes of this report, we simply note that the EMOX reactivity results are probably more robust in terms of their ability to predict relative trends than absolute values. They are not likely, though, to be more than a few percent in error.

Figure 3.7 Comparison of CASMO/HELIOS Reactivity Results for EMOX with 6 vol.% PuO_2, 1.5% Er_2O_3, and 70 vol.% Non-Fertile Material

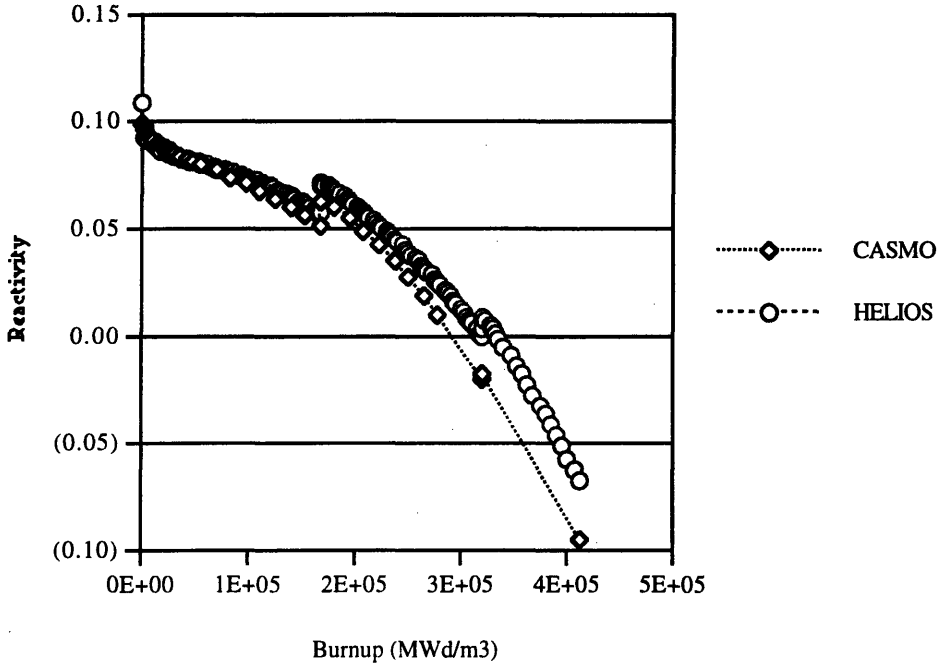

Table 3.10 HELIOS/CASMO-3 EOL Plutonium Isotopics for EMOX

Plutonium Isotope	HELIOS (kg/assembly)	CASMO-3 (kg/assembly)
Pu-238	0.39	0.27
Pu-239	4.35	3.81
Pu-240	4.46	4.73
Pu-241	3.41	3.26
Pu-242	2.64	2.04

3.3 Plutonium Destruction Capability of EMOX

The EMOX fuel concept is proposed as a plutonium management tool. It is important, therefore, to compare the amount and isotopic composition of the plutonium which results from the use of EMOX, UO_2, and MOX. This section focuses on the EMOX compositions which were found to have acceptable BOC and EOC reactivity as discussed in Section 3.2 (see Table 3.8). These compositions will be highlighted for easy

identification in tables throughout this section. Other compositions may be included in order to demonstrate and extend particular trends.

Table 3.11 gives the mass of fissile plutonium which is found in an assembly of a given EMOX composition before and after three 18 month irradiation cycles. Table 3.12 shows the same information for some MOX compositions and the reference UO_2 case. Of the five plutonium isotopes which were tracked in this work (Pu-238 through 242), only Pu-239 and Pu-241 are fissile. They are also, therefore, the isotopes which are most useful for constructing a nuclear weapon. It is apparent from Table 3.11 that variation of the EMOX erbia loading has little or no effect on the fuel's residual fissile plutonium content or, correspondingly, on its plutonium destruction capability. Increasing the initial fuel plutonium loading, however, tends to increase the amount of fissile plutonium in spent fuel while allowing for increased net fissile plutonium destruction. In the range of 3-6 vol.% initial PuO_2, an additional one volume percent PuO_2 (four to five kg fissile Pu per assembly) at BOL translates into about three more kilograms of fissile plutonium per assembly at EOL. In other words, approximately one to two of the added four or five kg/assembly of fissile plutonium will be destroyed.

Table 3.11 Mass of Fissile Plutonium in EMOX Compositions at BOL and EOL

30% Non-Fertile EMOX

Vol.% PuO_2	BOL Pu-fissile (kg/assembly)	EOL Pu-fissile (kg/assembly) by Volume Percent Er_2O_3 in EMOX Fuel 0.5%	1.0%	1.5%
4.0%	15.30	6.67 (56.4)	6.74 (55.9)	6.80 (55.6)
5.0%	19.12	9.36 (51.0)	9.43 (50.7)	9.50 (50.3)
6.0%	22.95	12.28 (46.5)	12.36 (46.1)	12.43 (45.8)

50% Non-Fertile EMOX

Vol.% PuO_2	BOL Pu-fissile (kg/assembly)	EOL Pu-fissile (kg/assembly) by Volume Percent Er_2O_3 in EMOX Fuel 0.5%	1.0%	1.5%
4.0%	15.30	4.70 (69.3)	4.74 (69.0	4.77 (68.8)
5.0%	19.12	7.30 (61.8)	7.34 (61.6)	7.39 (61.3)
6.0%	22.95	10.20 (55.6)	10.25 (65.3)	10.29 (55.2)

70% Non-Fertile EMOX

Vol.% PuO_2	BOL Pu-fissile (kg/assembly)	EOL Pu-fissile (kg/assembly) by Volume Percent Er_2O_3 in EMOX Fuel 0.5%	1.0%	1.5%
4.0%	15.30	2.52 (83.5)	2.51 (83.6)	2.51 (83.6)
5.0%	19.12	4.91 (74.3)	4.92 (74.3)	4.92 (74.3)
6.0%	22.95	7.75 (66.2)	7.76 (66.2)	7.76 (66.2)

Note: Shaded entries were deemed acceptable based on BOC and EOC reactivity criteria.
( ) = mass percent of Pu-fissile destroyed
Vol. % PuO_2 refers to total Pu; multiply by 0.7434 to get fissile Pu.

Table 3.12 Mass of Fissile Plutonium in MOX and UO_2 Compositions at BOL and EOL

	MOX Pu-fissile (kg/assembly)		UO_2 Pu-fissile (kg/assembly)	
Vol.% PuO_2	BOL	EOL	BOL	EOL
4.0%	15.30	9.22 (39.7)	0.0	2.89
5.0%	19.12	11.96 (37.4)		
6.0%	22.95	14.89 (35.1)		

Note: Shaded entries were deemed acceptable based on BOC and EOC reactivity criteria.
( ) = mass percent of Pu-fissile destroyed
Vol. % PuO_2 refers to total Pu; multiply by 0.7434 to get fissile Pu.

All of the selected EMOX cases have higher residual fissile plutonium amounts than the uranium fuel. The calculations show that a spent EMOX assembly will contain approximately two to four times the fissile plutonium of a spent uranium assembly. It should be noted, however, that the irradiation of a single EMOX assembly can destroy many times more fissile plutonium than is created in a uranium assembly. Comparison of residual Pu in MOX vs. that in EMOX is more relevant. Tables 3.11 and 3.12 demonstrate that MOX fuel is capable of destroying a significant fraction of its fissile plutonium loading (approximately 35-40% by mass), and that EMOX shows the potential for even greater plutonium reductions (approximately 46-84% destruction).

Comparing the results of EMOX cases with different NFPs demonstrates, as expected, that a higher non-fertile loading will lead to greater net fissile plutonium destruction. The absence of fertile U-238 which would otherwise have lead to additional fissile Pu-239 production reduces the amount of fissile material which remains after irradiation. Figure 3.8 shows the decrease in residual fissile plutonium, relative to MOX, which occurs with increasing NFP. The points in the figure were calculated by dividing the kilograms of fissile plutonium remaining in a given EMOX assembly at EOL by the kilograms of fissile plutonium at EOL in a comparable MOX assembly (one which had the same BOL PuO_2 loading as the EMOX). The fact that these ratios all come out to less than

100% indicates that all EMOX compositions have less EOL residual fissile plutonium and destroy more fissile plutonium than comparable MOX compositions. A line with a slope of negative one has been included in the graph for the sake of comparison. This line represents a one percent reduction in the fuel's EOL fissile plutonium for every volume percent of non-fertile material (which replaces fertile UO_2) in the initial fuel composition. One of the reasons that the EMOX compositions do not exhibit a one to one reduction is that the U-238 macroscopic capture cross section (capture leads to Pu-239 production) is proportional to the square root of the U-238 number density. The actual EMOX curves are nearly linear, but have slightly more negative slopes at higher NFPs. This indicates that plutonium destruction is somewhat more efficient at the higher non-fertile loadings.

Figure 3.8 Fissile Plutonium Remaining in EMOX as Compared to MOX for 1.5 vol.% Er_2O_3 EMOX Cases vs. Non-fertile Percentage

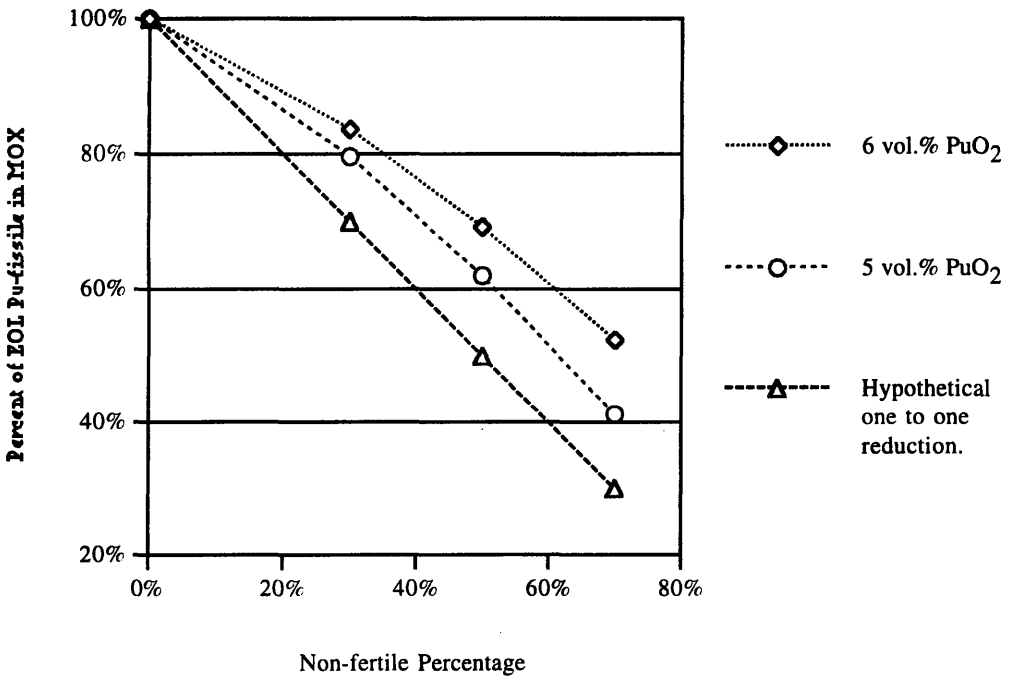

Note: MOX fuel is shown at 0% NFP.

Thus far, we have discussed only the fissile plutonium isotopes, neglecting Pu-238, 240, and 242. These isotopes are all less than ideal as materials for a nuclear weapon

[C-1]. Pu-238 can undergo spontaneous fission, which may reduce the yield of a nuclear explosive. It also decays via alpha emission, a reaction which produces a significant amount of decay heat and leads to handling difficulties. Pu-240 has a non-trivial (300 eV) threshold energy for fission, and Pu-242 has a large (100 keV) threshold. Pu-240 and 242 are also subject to spontaneous fission. These isotopes, while capable of sustaining nuclear chain reactions, are likely to detract from the weapons usability of plutonium. In examining the isotopic composition of the EMOX from a non-proliferation standpoint, therefore, the presence of large amounts of the even numbered plutonium isotopes relative to odd isotopes is considered desirable.

Table 3.13 gives the BOL plutonium isotopics for EMOX and MOX cases containing 4-6 vol.% PuO_2. These are included for comparison with Tables 3.14 and 3.15 which contain EOL plutonium isotopics for EMOX and MOX/UO_2 cases, respectively. Isotopic data is given only for promising EMOX compositions listed in Table 3.8. The data show that the amount of Pu-238 in an EMOX assembly is roughly the same before and after fuel irradiation. The Pu-239 content, by contrast, decreases significantly as much of it is fissioned. Pu-240 and 241 content tends to decrease modestly, while the amount of Pu-242 approximately doubles (though this only means an increase of about one kilogram).

Table 3.13 BOL Plutonium Isotopics for EMOX and MOX Compositions

PuO_2 Vol.%	(kg/assembly)					
	Pu-238	Pu-239	Pu-240	Pu-241	Pu-242	Total
4.0	0.24	12.31	4.15	2.99	0.90	20.58
5.0	0.30	15.38	5.18	3.74	1.13	25.72
6.0	0.35	18.46	6.22	4.49	1.35	30.87

Table 3.14 EOL EMOX Plutonium Isotopics

30% Non-Fertile EMOX

PuO_2 Vol.%	Er_2O_3 Vol.%	(kg/assembly) Pu-238	Pu-239	Pu-240	Pu-241	Pu-242	Total
4.0	0.5	0.28	4.23	3.28	2.44	2.13	12.35
		(2.26)	(34.25)	(26.56)	(19.76)	(17.25)	
	1.0	0.28	4.29	3.27	2.45	2.13	12.41
		(2.26)	(34.57)	(26.35)	(19.74)	(17.16)	
5.0	1.0	0.35	6.14	4.33	3.29	2.30	16.40
		(2.13)	(37.44)	(26.40)	(20.06)	(14.02)	
	1.5	0.35	6.20	4.31	3.30	2.29	16.45
		(2.13)	(37.69)	(26.20)	(20.06)	(13.92)	
6.0	1.5	0.41	8.35	5.38	4.08	2.46	20.68
		(1.98)	(40.38)	(26.02)	(19.73)	(11.90)	

50% Non-Fertile EMOX

PuO_2 Vol.%	Er_2O_3 Vol.%	(kg/assembly) Pu-238	Pu-239	Pu-240	Pu-241	Pu-242	Total
4.0	0.5	0.26	2.73	2.72	1.98	2.27	9.95
		(2.61)	(27.44)	(27.34)	(19.90)	(22.81)	
5.0	1.0	0.33	4.41	3.88	2.94	2.40	13.97
		(2.36)	(31.57)	(27.77)	(21.05)	(17.18)	
	1.5	0.33	4.44	3.87	2.95	2.40	13.99
		(2.36)	(31.74)	(27.66)	(21.09)	(17.16)	
6.0	1.5	0.40	6.47	5.02	3.82	2.54	18.25
		(2.19)	(35.45)	(27.51)	(20.93)	(13.92)	

70% Non-Fertile EMOX

PuO_2 Vol.%	Er_2O_3 Vol.%	(kg/assembly) Pu-238	Pu-239	Pu-240	Pu-241	Pu-242	Total
5.0	1.5	0.31	2.55	3.17	2.38	2.53	10.93
		(2.84)	(23.33)	(29.00)	(21.77)	(23.15)	

Note: ( ) = weight percent of total Pu
Vol. % PuO_2 refers to total Pu; multiply by 0.7434 to get fissile Pu.

Table 3.15 MOX and UO_2 EOL Plutonium Isotopics

MOX

PuO_2 Vol.%	Pu-238	Pu-239	Pu-240	Pu-241	Pu-242	Total
			(kg/assembly)			
4.0	0.29	6.36	3.82	2.86	2.00	15.32
	(1.89)	(41.51)	(24.93)	(18.67)	(13.05)	
5.0	0.36	8.36	4.80	3.60	2.19	19.30
	(1.87)	(43.32)	(24.87)	(18.65)	(11.35)	
6.0	0.42	10.58	5.81	4.31	2.38	23.49
	(1.79)	(45.04)	(24.73)	(18.35)	(10.13)	

UO_2

PuO_2 Vol.%	Pu-238	Pu-239	Pu-240	Pu-241	Pu-242	Total
			(kg/assembly)			
0.0	0.10	2.20	1.06	0.70	0.41	4.47
	(2.24)	(49.22)	(23.71)	(15.66)	(9.17)	

Note: ( ) = weight percent of total Pu
Vol. % PuO_2 refers to total Pu; multiply by 0.7434 to get fissile Pu.

The EOL EMOX plutonium isotopics do not vary significantly with changes in erbium loading. Increasing plutonium loadings, however, result in increasing absolute amounts of each isotope. Changes in NFP have different impacts on different isotopes, but the most notable result is a shift in the balance between fissile and non-fissile plutonium isotopes. As the NFP of EMOX is increased, small increases in EOL Pu-242 content are seen, as well as small decreases in Pu-240 content. The large reduction in fissile Pu-239, though, is overwhelmingly responsible for the relative isotopic shift. Figure 3.9 illustrates the increasing ratio of non-fissile to fissile plutonium in EMOX at EOL as a function of NFP. Note that the slope of the curve increases at higher non-fertile loadings. This indicates that a greater isotopic shift is accomplished per initial non-fertile fuel volume percent at higher non-fertile loadings. The figure also demonstrates that cases with lower plutonium loadings will have comparably higher non-fissile/fissile ratios. This is because a

larger fraction of fissile plutonium must be burned in fuels with less initial plutonium to achieve a specified burnup.

Figure 3.9 Ratio of Non-fissile to Fissile Plutonium at EOL vs. Non-fertile Percentage for MOX and 1.5 vol.% Er_2O_3 EMOX Cases

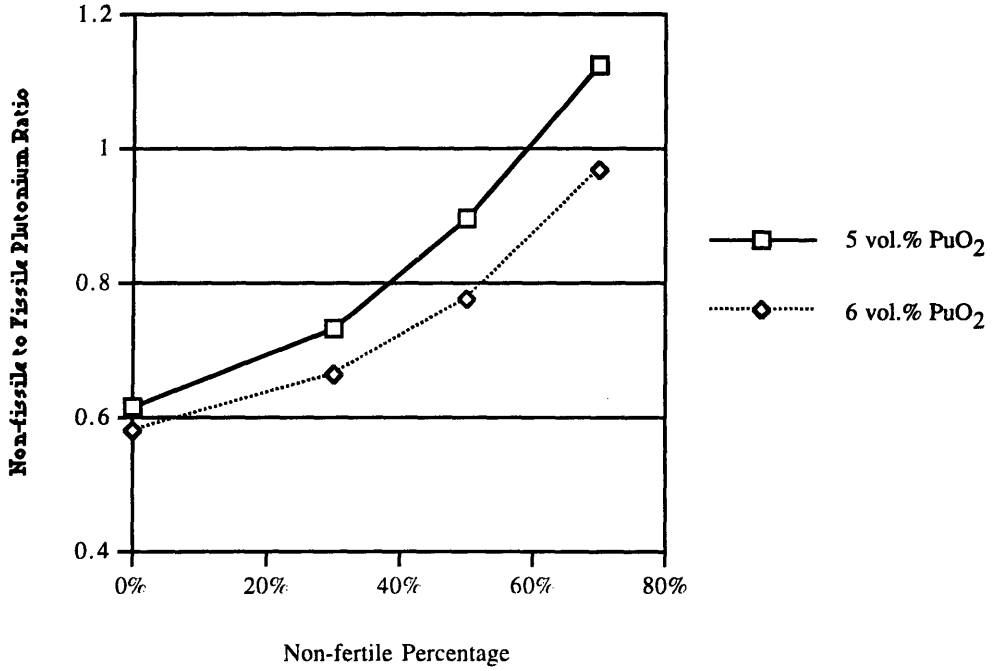

Note: MOX fuel is shown at 0% NFP.

As a final note, the yearly plutonium throughput and destruction amounts for some of the fuels we are concerned with bear mentioning. For the fuel compositions (MOX and EMOX) containing 5 vol.% PuO_2, an average of 1,097 kg of plutonium (816 kg of fissile Pu) per year are inserted into a single reactor core as fuel. Some fraction of this plutonium is fissioned or otherwise destroyed in the reactor and some is discharged in spent fuel. The total plutonium destruction (or production) rates for some EMOX cases of interest and the comparative MOX and UO_2 cases are found in Table 3.16. It is interesting to note that a single 5 vol.% PuO_2 assembly can incorporate an amount of plutonium equivalent to that produced in approximately nine standard uranium assemblies. That plutonium can then be to some degree "eliminated", depending on the chosen fuel composition. That is, some of

the plutonium is burned, while the remainder has degraded isotopics and is henceforth accompanied by a highly radioactive fission product inventory.

Table 3.16 Net Total Plutonium Destruction (Production) (kg per reactor year)

UO_2 (4.4 wt% U-235)	MOX (5 vol.% PuO_2)	EMOX (5 vol.% PuO_2, 1.5 vol.% Er_2O_3) 30 NFP	50 NFP	70 NFP
(123)	305	410	500	606

3.4 Summary

Several EMOX compositions with various PuO_2 loadings (3.0-6.0 vol.% total PuO_2), Er_2O_3 loadings (0.0-1.5 vol.%), and ZrO_2-CaO loadings (30-70 vol.%) have been examined with regard to their reactivity behavior and their plutonium destruction capability. The reactivity vs. burnup data at the beginning and end of each cycle are used to define BOC and EOC power weighted core average reactivity values for comparison with appropriate maximum and minimum criteria. A minimum EOC ρ_{core} of -0.05 was established as necessary for a given composition to remain critical throughout an 18-month cycle using soluble poison to simulate neutron losses by core leakage. A maximum BOL ρ_{core} of 0.06 was calculated, corresponding to the maximum amount of soluble boron which can be used in coolant without exceeding chemistry limits. Fuel compositions which were able to meet the BOC and EOC reactivity criteria are recommended for further study. None of the 3.0 vol.% PuO_2 cases or the 0.0 vol.% Er_2O_3 cases were selected. Of the remaining compositions , at least one was chosen at each PuO_2, ZrO_2-CaO, and Er_2O_3 loading. The reactivity vs. burnup behavior of the selected EMOX cases compares favorably with that of UO_2 fuel. The plutonium destruction capability of EMOX is shown to exceed that of MOX in all cases. Plutonium destruction, both net and percentage, is increased as more non-fertile material is used in the fuel. The isotopic content of plutonium in the spent EMOX fuel is also favorably affected by higher ZrO_2-CaO loadings in that the ratio of non-fissile to fissile plutonium is increased.

CHAPTER FOUR: CONCLUSIONS

4.1 Introduction

This work explores the performance of evolutionary mixed-oxide (EMOX) fuel as a tool for more efficient consumption of plutonium. EMOX is a mixture of traditional MOX fuel with a neutronically inert component (in this case calcia-stabilized zirconia). In addition, erbia may also be employed homogeneously to hold down excess reactivity. The immediate advantage of such a fuel is the reduction of in-core plutonium production (as compared to standard UO_2 or MOX fuels) due to replacement of some fraction of fertile U-238 with non-fertile material. The use of full core EMOX would allow net RGP stockpile reductions. At the extreme, 100% replacement of the UO_2 component eliminates in-core plutonium production. EMOX is intended to serve as an intermediate evolutionary step between current commercial uranium fuels and non-uranium fuels. Initially, EMOX fuels containing small amounts of non-fertile material would have properties very similar to current fuels and thus be comparatively easy to license. The addition of incrementally greater amounts of non-fertile material to EMOX compositions could then ease the transition to fully non-fertile fuels, answering many of the requisite technical questions along the way.

This work is an initial survey of the performance of various EMOX compositions and is aimed at selecting those cases which seem most promising for further study. A model of a single Westinghouse PWR assembly was developed using the HELIOS code to simulate the irradiation of each fuel composition through three 18 calendar month cycles. A method was developed to simulate whole-core effects (power history and leakage) using HELIOS output. In Sections 4.2 and 4.3, notable results of these simulations are reviewed. Trends in the reactivity behavior and plutonium destruction capability of EMOX as a function of PuO_2, Er_2O_3, and non-fertile loadings are cited followed by a discussion of the merits of the recommended EMOX cases. Finally, there are many additional issues which must be addressed before EMOX could be used in commercial nuclear reactors. Important examples of these tasks are described in Section 4.4.

4.2 Trends Among EMOX Compositions

Several trends must be considered when designing an EMOX composition to meet specific assembly and core reactivity requirements. The two most obvious trends are the increase in reactivity which accompanies increasing plutonium loadings and the reactivity decrease due to the presence of erbia. The effects of both of these materials is found throughout the lifetime of the fuel, but may be more or less important at different times. Figure 4.1 shows the variation in Pu-239 and Er-167 number densities over the course of fuel lifetime for an example EMOX case. An increase in plutonium loading will cause an increase in BOL and EOL reactivity, but the effect will be more pronounced at EOL. Conversely, erbia has a larger negative reactivity impact at BOL and burns out over the course of the first cycle to a minimal residual level. Erbia can be added to bring down excess peak reactivity, but the EOL residual erbium in the fuel may in turn make it difficult for a core to sustain its desired cycle length. The plutonium and erbium fuel components must be balanced such that there is enough fissile material for the core to remain critical for

the prescribed cycle length, but not so much that the peak core reactivity is beyond allowable limits.

Figure 4.1 Pu-239 and Er-167 Number Densities vs. Burnup for EMOX Case 1.5 vol.% Er_2O_3, 6 vol.% PuO_2, and 70 NFP

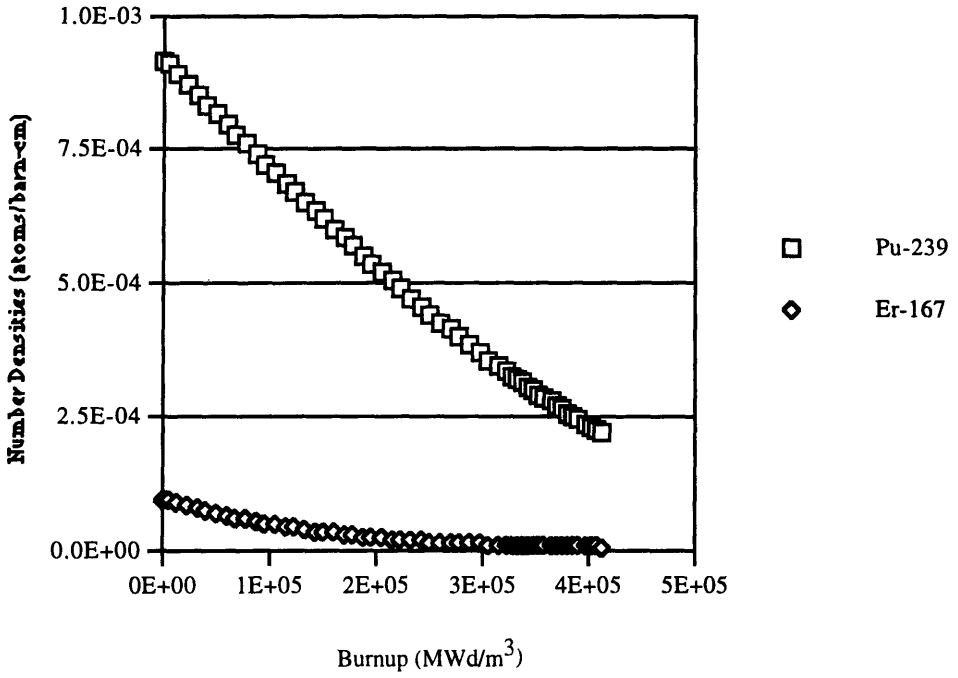

The non-fertile percentage (NFP) of the fuel also affects reactivity. Fuels with higher NFPs have higher BOC core average reactivities, for comparable plutonium and erbium loadings, due to the reduction in absorption by U-238. The absence of the fertile U-238, however, results in less Pu-239 production and generally lower EOC core averaged reactivity. Figure 4.2 demonstrates that at or below PuO_2 loadings of 5 vol.%, increasing NFPs decrease EOC power weighted core average reactivities. The figure also shows that this trend weakens with increasing plutonium loadings until, at 6 vol.% PuO_2, slight increases in the EOC ρ_{core} vs. NFP are observed. This shift is due to the balance between

increasing reactivity due to more plutonium and the NFP reactivity effects described above. It seems likely, therefore, that EOC core reactivities would also continue to increase with NFP at higher plutonium loadings.

Figure 4.2 Excess Core Averaged Reactivity at EOC vs. Fuel Non-Fertile Loading for EMOX Cases with 1.5 vol.% Er_2O_3

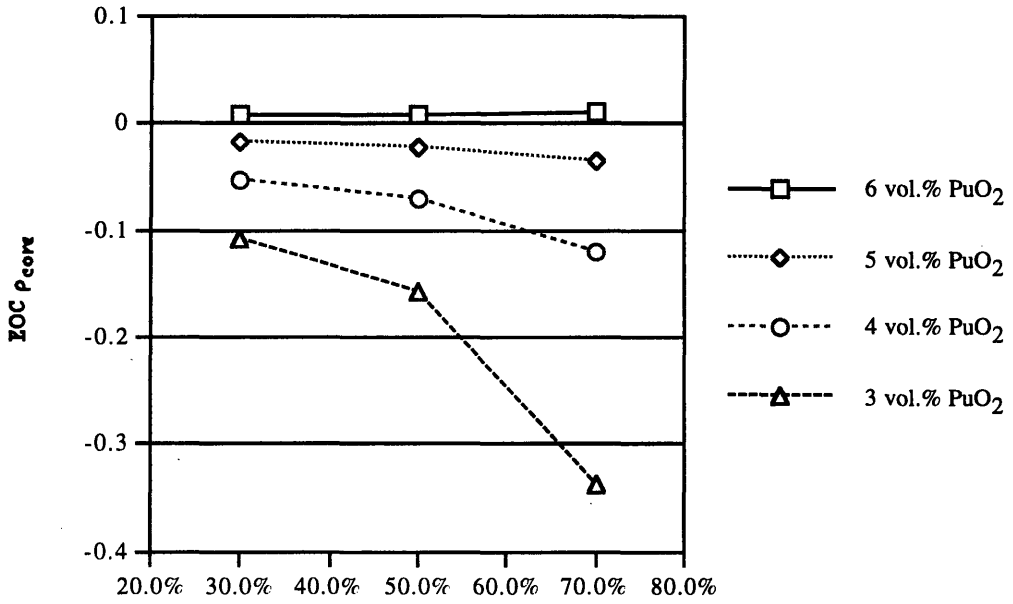

EMOX plutonium destruction capability and residual isotopic composition varies as a function of NFP and plutonium loading. These trends can be used as a guide in finding an EMOX composition which produces acceptable plutonium residual levels. Increasing fuel plutonium loading increases the net amount of plutonium per fuel assembly which is destroyed. It also increases residual plutonium levels in the spent fuel, and results in the destruction of a smaller percentage of the fuel's initial plutonium. Increasing the NFP has the desirable effects of increasing net and percentage of plutonium destruction while

decreasing residual plutonium. Table 4.1 demonstrates the fissile and total plutonium destruction capability of EMOX as compared to MOX. The table lists the ratios of percent plutonium destruction (by weight) in EMOX compositions to that in MOX compositions with identical initial PuO_2 loadings. In all cases, this ratio is greater than one, which indicates that EMOX of any composition will destroy more plutonium than its MOX counterpart. In some cases, EMOX plutonium destruction is more than twice that of MOX.

Table 4.1 Plutonium Destruction Capability of Selected EMOX Compositions (as Compared to MOX)

30% Non-Fertile EMOX

PuO_2 Vol.%	Er_2O_3 Vol.%	(wt% Pu destroyed in EMOX / wt% Pu destroyed in MOX) Fissile Pu	Total Pu
4.0	0.5	1.42	1.56
	1.0	1.41	1.55
5.0	1.0	1.36	1.45
	1.5	1.34	1.44
6.0	1.5	1.30	1.38

50% Non-Fertile EMOX

PuO_2 Vol.%	Er_2O_3 Vol.%	(wt% Pu destroyed in EMOX / wt% Pu destroyed in MOX) Fissile Pu	Total Pu
4.0	0.5	1.75	2.02
5.0	1.0	1.65	1.83
	1.5	1.64	1.82
6.0	1.5	1.57	1.71

70% Non-Fertile EMOX

PuO_2 Vol.%	Er_2O_3 Vol.%	(wt% Pu destroyed in EMOX / wt% Pu destroyed in MOX) Fissile Pu	Total Pu
5.0	1.5	1.99	2.30

Note: Vol. % PuO_2 refers to total Pu; multiply by 0.7434 to get fissile Pu.
EMOX compositions in this table were deemed acceptable based on BOC and EOC reactivity criteria.

The plutonium destruction performance of EMOX improves with increasing NFPs. Figure 4.3 shows that higher NFPs also produce an increase in the ratio of non-fissile to fissile plutonium in the resulting spent fuel, making the residual plutonium less attractive for weapons use. Pure MOX compositions are shown in Figure 4.3 at 0% NFP.

Figure 4.3 Ratio of Non-fissile to Fissile Plutonium at EOL vs. Non-fertile Percentage for MOX and 1.5 vol.% Er_2O_3 EMOX Cases

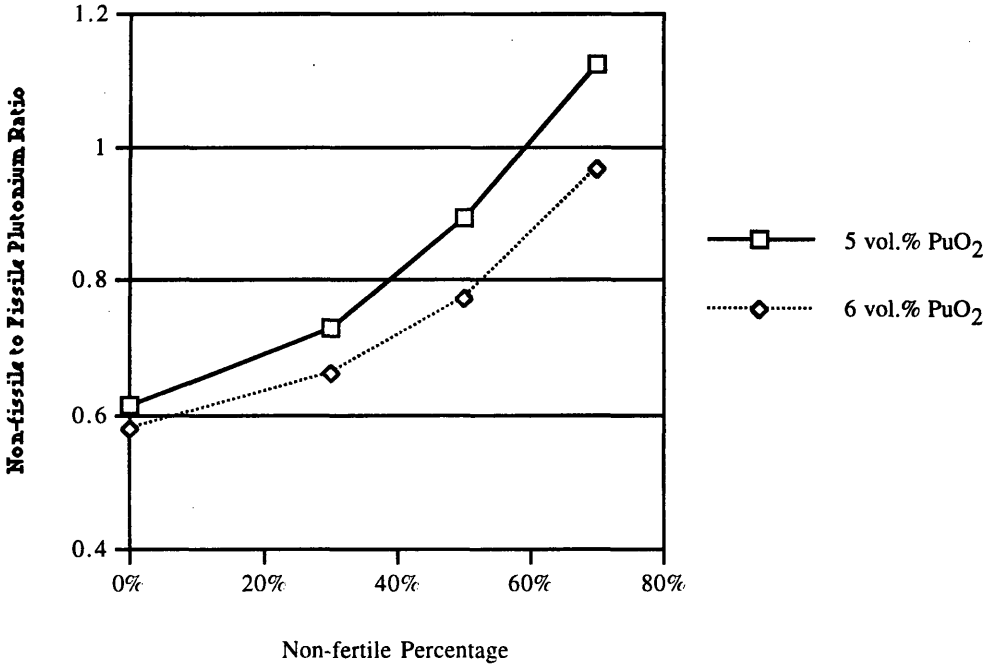

4.3 Promising EMOX Compositions

This preliminary analysis has shown that there are EMOX compositions which, when used to fully load a PWR core, can sustain an 18-month fuel cycle without exceeding basic peak reactivity limits. The reactivity behavior of these compositions as a function of burnup is comparable to that of standard UO_2 fuel. In addition, these fuels demonstrate an ability to destroy more plutonium than comparable MOX fuels, thereby leaving less residual plutonium in their spent fuel. An EMOX assembly also can easily destroy an

amount of plutonium equivalent to that produced during irradiation of a standard uranium assembly. Thus the use of full core EMOX would allow net RGP stockpile reductions. Table 4.2 gives plutonium destruction data for a subset of the chosen EMOX compositions. The 5 vol.% PuO_2, 1.5 vol.% Er_2O_3 cases are the only ones to have been deemed acceptable based on reactivity criteria at all of the NFPs which were investigated. This data demonstrates the validity of the many of the above conclusions .

Table 4.2 Plutonium Destruction Data for Selected EMOX and MOX Compositions and the Reference UO_2 Case

Composition **EMOX:**	BOL Pu-total (kg/assembly)	EOL Pu-total (kg/assembly)	Δ Pu-total (kg/assembly)	% Pu-total Destroyed (EOL kg/BOL kg)
30 NFP	25.72	16.45	-9.27	36.0
50 NFP	25.72	13.99	-11.73	45.6
70 NFP	25.72	10.93	-14.79	57.5
MOX	25.72	19.30	-6.42	25.0
UO_2	0.0	4.47	4.47	----

Note: All listed EMOX compositions contained 5 vol.% PuO_2, 1.5 vol.% Er_2O_3. The MOX composition also contained 5 vol.% PuO_2.

EMOX compositions were recommended for further study if they had acceptable BOC and EOC core average reactivity values. The rejected cases were either too reactive at BOC or not reactive enough at EOC to keep a core critical. All of the compositions containing 3 vol.% PuO_2 were not reactive enough to meet the EOC criteria, while all of the 0.0 vol.% Er_2O_3 cases had BOC core reactivities which were too high to be acceptable. None of the other plutonium or erbium compositions were entirely rejected. A full list of acceptable cases appears in Table 4.3. It should be noted that there are likely to be additional worthy EMOX compositions with higher plutonium and erbium loadings at all

NFPs. Based on the results of this work, it is recommended that EMOX cases which are similar in composition to those in Table 4.3 be the starting point for future investigations.

Table 4.3 EMOX Compositions Recommended for Further Study

PuO_2 Vol.%	Er_2O_3 Vol.%
30% Non-fertile	
4.0	0.5
	1.0
5.0	1.0
	1.5
6.0	1.5
50% Non-fertile	
4.0	0.5
5.0	1.0
	1.5
6.0	1.5
70% Non-fertile	
5.0	1.5

4.4 Future Work

The EMOX compositions surveyed in this work were judged principally on BOC and EOC core average reactivity values. These criteria are only rough estimates of the adequacy of in-core fuel neutronic performance. The next steps in evaluating EMOX as a fuel concept will involve more extensive neutronic calculations, including the investigation of reactor safety coefficients. Moderator temperature and void coefficients need to be studied, though the presence of erbia in the fuel may help insure that these coefficients are negative. The addition of other burnable poisons, such as gadolinium or boron, may be

considered to displace additional soluble poison and/or better control local assembly reactivity (and hence power) over a burnup cycle. Doppler coefficients are reduced in fuels with lowered U-238 content, such as EMOX, and plutonium containing fuels are known to decrease control rod worth as compared to uranium fuels. These facts may prove problematic, therefore, and need to be determined for various EMOX compositions. Assembly and pin power peaking factors will also need to be examined for realistic power histories and core loadings.

Eventually, true full core simulations of promising EMOX compositions will be necessary for a licensing-level qualification of many neutronic and thermal hydraulic parameters. The HELIOS code does not in and of itself have the ability to do a full 3-D core simulation. Thus, it will need to be allied with other simulation tools for advanced investigations. Finally, although it has been examined by others, the 100% non-fertile case should be included in future EMOX studies to provide data for inter-laboratory comparison and to establish the outer envelope of EMOX capabilities as a plutonium elimination tool.

There are also materials issues surrounding the addition of an inert matrix to MOX fuel which need to be addressed. Zirconia, specifically, has a lower thermal conductivity than uranium oxide, and there is concern over its ability to transfer sufficient heat out of fuel rods at acceptable fuel centerline temperatures [C-1]. EMOX fabrication is believed to be possible using techniques very similar to those currently in use in commercial fuel fabrication facilities [B-3]. Experimentation to verify fabrication processes, however, is still underway.

4.5 Summary

This work has documented basic trends in the reactivity behavior and plutonium destruction capability of EMOX fuels as a function of their initial composition. It has been shown that EMOX is a more effective plutonium destruction tool than standard MOX, and

that the reactivity behavior of selected compositions roughly approximates that of typical uranium fuels. On this basis, the EMOX concept appears to be a viable approach to plutonium management. Based on the results of these investigations, a specific set of EMOX compositions has been recommended for further study.

Appendix A Nomenclature

BOC	beginning of cycle
CaO	calcia
CISAC	Committee on International Security and Arms Control
EMOX	evolutionary mixed-oxide
EOC	end of cycle
Er	erbium
Er_2O_3	erbia
INEEL	Idaho National Engineering and Environmental Laboratory
k_{eff}	k-effective
LANL	Los Alamos National Laboratory
LHGR	linear heat generation rate
LWR	light water reactor
MOX	mixed-oxide
MT	metric tons
NAS	National Academy of Sciences
NFF	non-fertile fuel
NFP	non-fertile percentage
PNL	Pacific Northwest Laboratories
Pu	plutonium
PuO_2	plutonia
PWR	pressurized water reactor
RGP	reactor grade plutonium
ThO_2	thoria
U	uranium
UO_2	urania

Vol.%	volume percent
WGP	weapons grade plutonium
wt%	weight percent
ZrO_2	zirconia

Appendix B Figures Showing HELIOS Models of PNL Lattices 31-35

Figure B.1 HELIOS Model of Lattice PNL-31

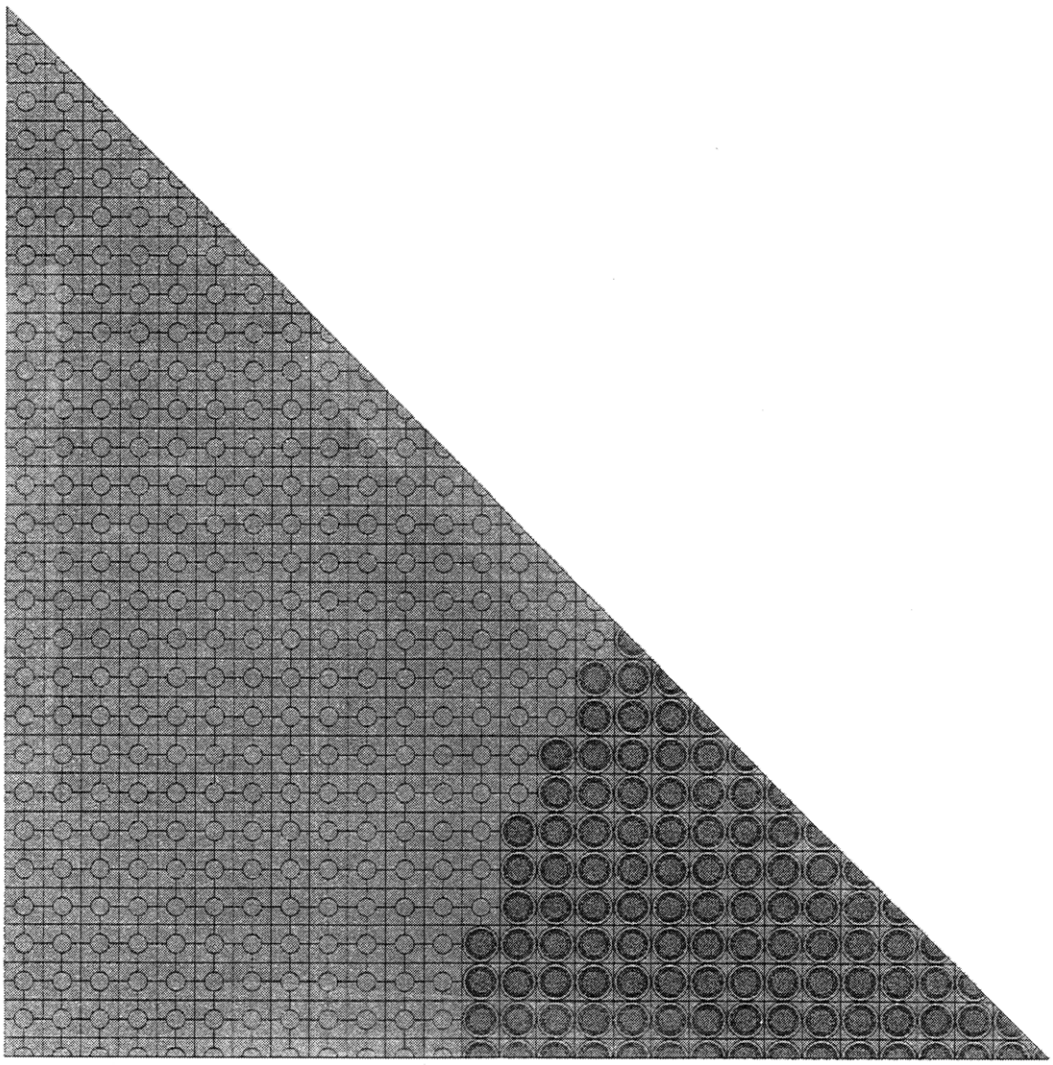

Squares containing dark inner circles are fuel pin cells. All other squares are moderator regions (divided into five subregions). The figure is drawn to scale. One inch on the page represents 9.00 cm. The exact geometry used in all HELIOS benchmark calculations can be inferred from the HELIOS input files. These can be obtained from Prof. M. J. Driscoll of the MIT Nuclear Engineering Department.

Figure B.2 HELIOS Model of Lattice PNL-32

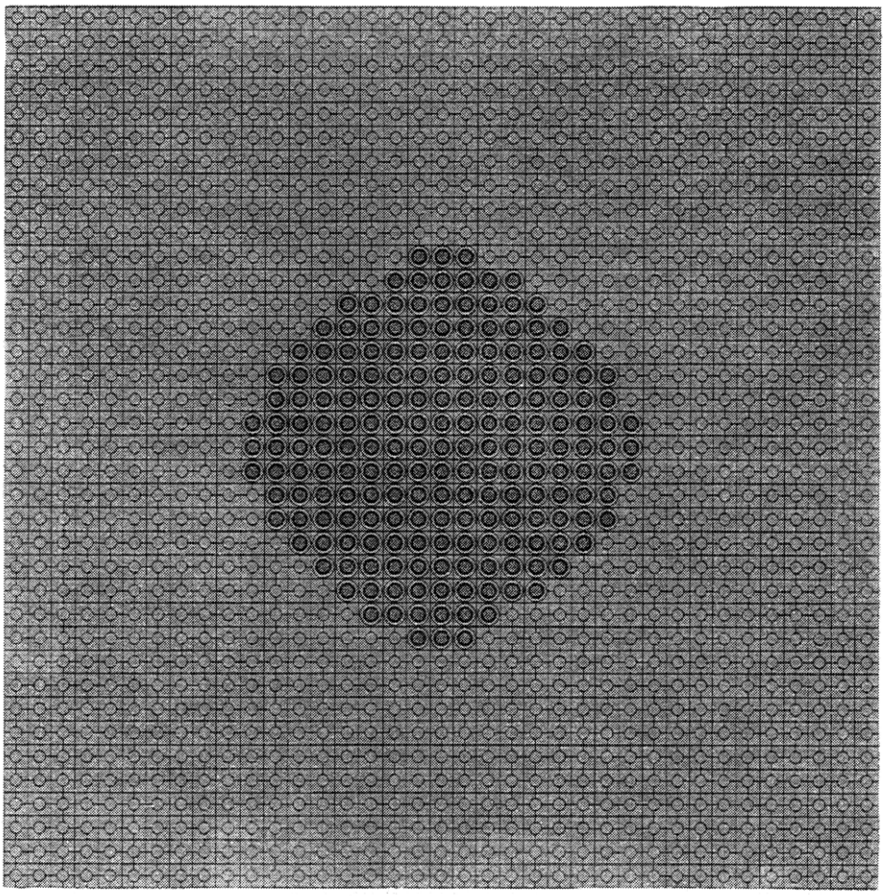

Squares containing dark inner circles are fuel pin cells. All other squares are moderator regions (divided into five subregions). The figure is drawn to scale. One inch on the page represents 18.21 cm.

Figure B.3 HELIOS Model of Lattice PNL-34

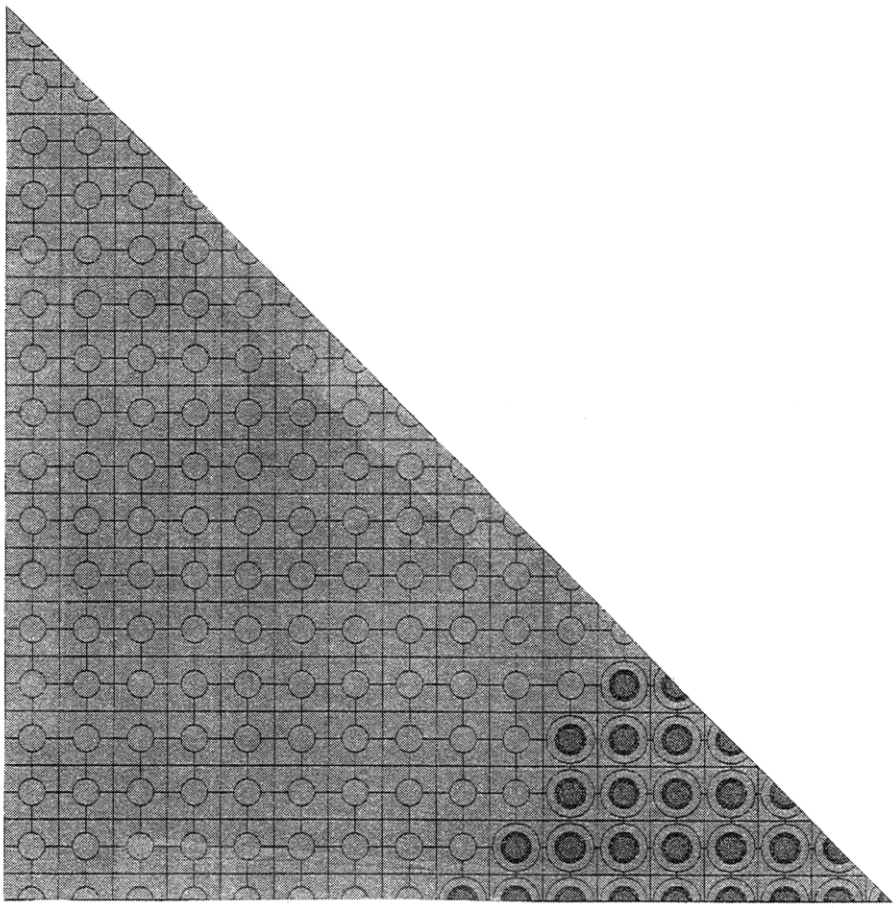

Squares containing dark inner circles are fuel pin cells. All other squares are moderator regions (divided into five subregions). The figure is drawn to scale. One inch on the page represents 9.00 cm.

Figure B.4 HELIOS Model of Lattice PNL-35

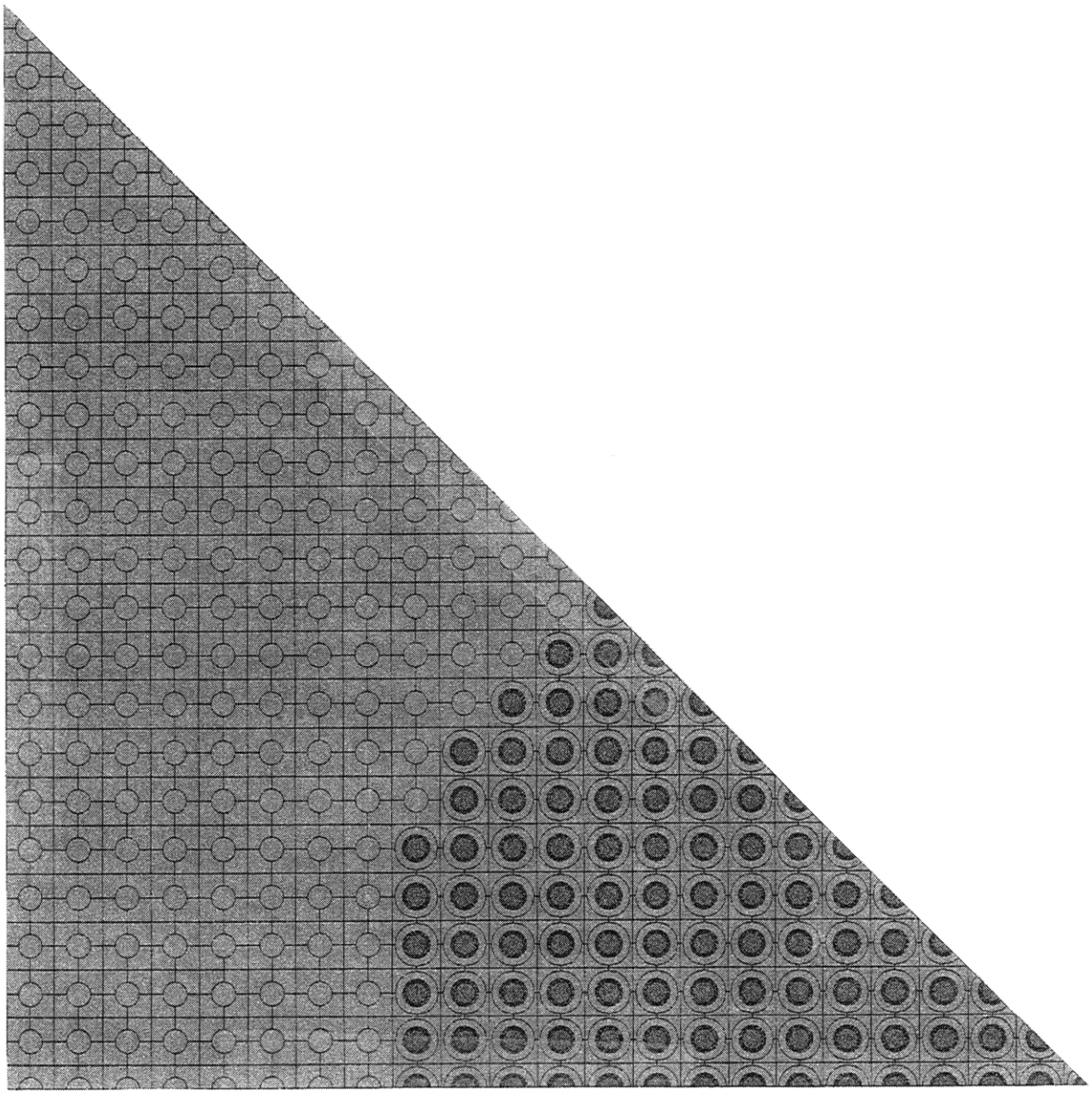

Squares containing dark inner circles are fuel pin cells. All other squares are moderator regions (divided into five subregions). The figure is drawn to scale. One inch on the page represents 9.11 cm.

Appendix C Sample HELIOS (AURORA) and CASMO-3 Input Files

Sample HELIOS (AURORA) Input:

```
+HELIOS
'6p70nf15'      =CASE ( 'lib34' / '6p70nf15.hrf'/ '6p70nf15' )

!234567892234567893234567894234567895234567896234567897234567897234567897234567897
!

!*******************Materials Specification**************************!

fuel        =MAT ( / 92235, 3.8933E-5; 92238, 5.4616E-3; 94238,
                     1.7636E-5; 94239, 9.1386E-4; 94240, 3.0660E-4;
                     94241, 2.2038E-4; 94242, 6.6040E-5; 40000,
                     1.6284E-2; 20000, 3.7377E-3; 8016, 5.0355E-2;
                     68166, 1.4520E-4; 68167, 9.3777E-5; 68168,
                     1.0894E-4; 68170, 5.9942E-5 )

clad        =MAT ( / 40002, 3.7376E-2 )

mod1        =MAT ( NB // 1001, 4.3093E-2; 8016, 2.1547E-2; 5010,
                     5.3542E-6; 5011, 2.1552E-5 )

mod2        =MAT ( NB // 1001, 4.7331E-2; 8016, 2.3665E-2; 5010,
                     5.8808E-6; 5011, 2.3671E-5 )

mod3        =MAT ( NB // 1001, 4.8779E-2; 8016, 2.4390E-2; 5010,
                    6.0607E-6; 5011, 2.4395E-5 )

!********************** Define Parameters ******************************!

$k          =PAR ( 4 )

$hp         =PAR ( "0.62992" )      ! half pitch !

$rmod       =PAR ( "0.60448" )     ! rad. of fuel pin mod. ring !

$rclad      =PAR ( "0.60198" )     ! rad. of clad in coolant channels !

$space      =PAR ( "0.0435" )

$pitch      =PAR ( "1.2598" )

!********************** System Components ******************************!

fuelpin      =CCS ( 0.14481, 0.20479, 0.25081, 0.28961, 0.32380,
```

```
                0.35470, 0.38312, 0.409575, 0.47498,
                $rmod / / fuel1, fuel2, fuel3, fuel4, fuel5,
                fuel6, fuel7, fuel8, clad, mod )

coolchn     =CCS ( 0.28067, 0.39693, 0.486135, 0.56134, $rclad
                / / cool1, cool2, cool3, cool4, clad )

pincell     =STR ( ( "-$hp", $hp )  ( $hp, $hp )
                ( $hp, "-$hp" )  ( "-$hp", "-$hp" )
                ( 0.0, $hp )  ( $hp, 0.0 )
                ( 0.0, "-$hp" )  ( "-$hp", 0.0 )
                ( 0.0, $rmod )  ( $rmod, 0.0 )
                ( 0.0, "-$rmod" )  ( "-$rmod", 0.0 )
                / 4, SWmod/ fuelpin ( 0.0, 0.0 ) /
                1, 5, 9, 12, 8, NWmod; 5, 2, 6, 10, 9,
                NEmod; 10, 6, 3, 7, 11, SEmod )

coolcell    =STR ( ( "-$hp", $hp )  ( $hp, $hp )
                ( $hp, "-$hp" )  ( "-$hp", "-$hp" )
                ( 0.0, $hp )  ( $hp, 0.0 )
                ( 0.0, "-$hp" )  ( "-$hp", 0.0 )
                ( 0.0, $rclad )  ( $rclad, 0.0 )
                ( 0.0, "-$rclad" )  ( "-$rclad", 0.0 )
                / 4, SWmod/ coolchn ( 0.0, 0.0 ) /
                1, 5, 9, 12, 8, NWmod; 5, 2, 6, 10, 9,
                NEmod; 10, 6, 3, 7, 11, SEmod )

 spacer     =STR ( ( 0.0, $space )  ( $pitch, $space )
                ( $pitch,  0.0 )  ( 0.0, 0.0 ) / 4,
                h2o / / )

square      =STR ( ( 0.0, $space )  ( $space, $space )
                ( $space,  0.0 )  ( 0.0, 0.0 ) / 4,
                h2o / / )

!-------------------Whole Assembly Rows-------------------------!

spacerow    =CNX ( square, spacer, spacer, spacer, spacer,
                 spacer, spacer, spacer, spacer, spacer,
                 spacer, spacer, spacer, spacer, spacer,
                 spacer, spacer, spacer, square / ( 1, 2, 3 )
                $k ( 2, 1, 4 ) / ( 2, 2, 3 ) $k ( 3, 1, 4 ) /
                ( 3, 2, 3 ) $k ( 4, 1, 4 ) / ( 4, 2, 3 ) $k
                ( 5, 1, 4 ) / ( 5, 2, 3 ) $k ( 6, 1, 4 ) /
                ( 6, 2, 3 ) $k ( 7, 1, 4 ) / ( 7, 2, 3 ) $k
                ( 8, 1, 4 ) / ( 8, 2, 3 ) $k ( 9, 1, 4 ) /
                ( 9, 2, 3 ) $k ( 10, 1, 4 ) / ( 10, 2, 3 ) $k
                ( 11, 1, 4 ) / ( 11, 2, 3 ) $k ( 12, 1, 4 ) /
                ( 12, 2, 3 ) $k ( 13, 1, 4 ) / ( 13, 2, 3 ) $k
                ( 14, 1, 4 ) / ( 14, 2, 3 ) $k ( 15, 1, 4 ) /
                ( 15, 2, 3 ) $k ( 16, 1, 4 ) / ( 16, 2, 3 ) $k
                ( 17, 1, 4 ) / ( 17, 2, 3 ) $k ( 18, 1, 4 ) /
                ( 18, 2, 3 ) $k ( 19, 1, 4 ) )
```

```
fuelrow      =CNX ( spacer, pincell, pincell, pincell, pincell,
                    pincell, pincell, pincell, pincell, pincell,
                    pincell, pincell, pincell, pincell, pincell,
                    pincell, pincell, pincell, spacer / ( 1, 1,
                   2 ) $k ( 2, 1, 4 ) / ( 2, 2, 3 ) $k ( 3, 1, 4 )
                   / ( 3, 2, 3 ) $k ( 4, 1, 4 ) / ( 4, 2, 3 ) $k
                   ( 5, 1, 4 ) / ( 5, 2, 3 ) $k ( 6, 1, 4 ) /
                   ( 6, 2, 3 ) $k ( 7, 1, 4 ) / ( 7, 2, 3 ) $k
                   ( 8, 1, 4 ) / ( 8, 2, 3 ) $k ( 9, 1, 4 ) /
                   ( 9, 2, 3 ) $k ( 10, 1, 4 ) / ( 10, 2, 3 ) $k
                   ( 11, 1, 4 ) / ( 11, 2, 3 ) $k ( 12, 1, 4 ) /
                   ( 12, 2, 3 ) $k ( 13, 1, 4 ) / ( 13, 2, 3 ) $k
                   ( 14, 1, 4 ) / ( 14, 2, 3 ) $k ( 15, 1, 4 ) /
                   ( 15, 2, 3 ) $k ( 16, 1, 4 ) / ( 16, 2, 3 ) $k
                   ( 17, 1, 4 ) / ( 17, 2, 3 ) $k ( 18, 1, 4 ) /
                   ( 18, 2, 3 ) $k ( 19, 4, 3 ) )

'3coolrow'   =CNX ( spacer, pincell, pincell, pincell, pincell,
                    pincell, coolcell, pincell, pincell, coolcell,
                    pincell, pincell, coolcell, pincell, pincell,
                    pincell, pincell, pincell, spacer / ( 1, 1,
                   2 ) $k ( 2, 1, 4 ) / ( 2, 2, 3 ) $k ( 3, 1, 4 )
                   / ( 3, 2, 3 ) $k ( 4, 1, 4 ) / ( 4, 2, 3 ) $k
                   ( 5, 1, 4 ) / ( 5, 2, 3 ) $k ( 6, 1, 4 ) /
                   ( 6, 2, 3 ) $k ( 7, 1, 4 ) / ( 7, 2, 3 ) $k
                   ( 8, 1, 4 ) / ( 8, 2, 3 ) $k ( 9, 1, 4 ) /
                   ( 9, 2, 3 ) $k ( 10, 1, 4 ) / ( 10, 2, 3 ) $k
                   ( 11, 1, 4 ) / ( 11, 2, 3 ) $k ( 12, 1, 4 ) /
                   ( 12, 2, 3 ) $k ( 13, 1, 4 ) / ( 13, 2, 3 ) $k
                   ( 14, 1, 4 ) / ( 14, 2, 3 ) $k ( 15, 1, 4 ) /
                   ( 15, 2, 3 ) $k ( 16, 1, 4 ) / ( 16, 2, 3 ) $k
                   ( 17, 1, 4 ) / ( 17, 2, 3 ) $k ( 18, 1, 4 ) /
                   ( 18, 2, 3 ) $k ( 19, 4, 3 ) )

'2coolrow'   =CNX ( spacer, pincell, pincell, pincell, coolcell,
                    pincell, pincell, pincell, pincell, pincell,
                    pincell, pincell, pincell, pincell, coolcell,
                    pincell, pincell, pincell, spacer / ( 1, 1,
                   2 ) $k ( 2, 1, 4 ) / ( 2, 2, 3 ) $k ( 3, 1, 4 )
                   / ( 3, 2, 3 ) $k ( 4, 1, 4 ) / ( 4, 2, 3 ) $k
                   ( 5, 1, 4 ) / ( 5, 2, 3 ) $k ( 6, 1, 4 ) /
                   ( 6, 2, 3 ) $k ( 7, 1, 4 ) / ( 7, 2, 3 ) $k
                   ( 8, 1, 4 ) / ( 8, 2, 3 ) $k ( 9, 1, 4 ) /
                   ( 9, 2, 3 ) $k ( 10, 1, 4 ) / ( 10, 2, 3 ) $k
                   ( 11, 1, 4 ) / ( 11, 2, 3 ) $k ( 12, 1, 4 ) /
                   ( 12, 2, 3 ) $k ( 13, 1, 4 ) / ( 13, 2, 3 ) $k
                   ( 14, 1, 4 ) / ( 14, 2, 3 ) $k ( 15, 1, 4 ) /
                   ( 15, 2, 3 ) $k ( 16, 1, 4 ) / ( 16, 2, 3 ) $k
                   ( 17, 1, 4 ) / ( 17, 2, 3 ) $k ( 18, 1, 4 ) /
                   ( 18, 2, 3 ) $k ( 19, 4, 3 ) )

'5coolrow'   =CNX ( spacer, pincell, pincell, coolcell, pincell,
                    pincell, coolcell, pincell, pincell, coolcell,
```

```
                    pincell, pincell, coolcell, pincell, pincell,
                    coolcell, pincell, pincell, spacer / ( 1, 1,
                   2 ) $k ( 2, 1, 4 ) / ( 2, 2, 3 ) $k ( 3, 1, 4 )
                   / ( 3, 2, 3 ) $k ( 4, 1, 4 ) / ( 4, 2, 3 ) $k
                   ( 5, 1, 4 ) / ( 5, 2, 3 ) $k ( 6, 1, 4 ) /
                   ( 6, 2, 3 ) $k ( 7, 1, 4 ) / ( 7, 2, 3 ) $k
                   ( 8, 1, 4 ) / ( 8, 2, 3 ) $k ( 9, 1, 4 ) /
                   ( 9, 2, 3 ) $k ( 10, 1, 4 ) / ( 10, 2, 3 ) $k
                   ( 11, 1, 4 ) / ( 11, 2, 3 ) $k ( 12, 1, 4 ) /
                   ( 12, 2, 3 ) $k ( 13, 1, 4 ) / ( 13, 2, 3 ) $k
                   ( 14, 1, 4 ) / ( 14, 2, 3 ) $k ( 15, 1, 4 ) /
                   ( 15, 2, 3 ) $k ( 16, 1, 4 ) / ( 16, 2, 3 ) $k
                   ( 17, 1, 4 ) / ( 17, 2, 3 ) $k ( 18, 1, 4 ) /
                   ( 18, 2, 3 ) $k ( 19, 4, 3 ) )

fullasmb     =CNX ( spacerow, fuelrow, fuelrow, '3coolrow',
                   '2coolrow', fuelrow, '5coolrow', fuelrow,
                   fuelrow, '5coolrow', fuelrow, fuelrow,
                   '5coolrow', fuelrow, '2coolrow', '3coolrow',
                   fuelrow, fuelrow, spacerow / ( 1-1, 3, 4 )
                   $k ( 2-1, 1, 4 ) / ( 2-1, 2, 3 ) $k ( 3-1,
                   1, 4 ) / ( 3-1, 2, 3 ) $k ( 4-1, 1, 4 ) /
                   ( 4-1, 2, 3 ) $k ( 5-1, 1, 4 ) / ( 5-1, 2, 3 )
                   $k ( 6-1, 1, 4 ) / ( 6-1, 2, 3 ) $k ( 7-1, 1,
                   4 ) / ( 7-1, 2, 3 ) $k ( 8-1, 1, 4 ) / ( 8-1,
                   2, 3 ) $k ( 9-1, 1, 4 ) / ( 9-1, 2, 3 ) $k
                   ( 10-1, 1, 4 ) / ( 10-1, 2, 3 ) $k ( 11-1, 1,
                   4 ) / ( 11-1, 2, 3 ) $k ( 12-1, 1, 4 ) /
                   ( 12-1, 2, 3 ) $k ( 13-1, 1, 4 ) / ( 13-1, 2,
                   3 ) $k ( 14-1, 1, 4 ) / ( 14-1, 2, 3 ) $k
                   ( 15-1, 1, 4 ) / ( 15-1, 2, 3 ) $k ( 16-1, 1,
                   4 ) / ( 16-1, 2, 3 ) $k ( 17-1, 1, 4 ) /
                   ( 17-1, 2, 3 ) $k ( 18-1, 1, 4 ) / ( 18-1, 2,
                   3 ) $k ( 19-1, 2, 1 ) )

system     =CNX ( fullasmb )

!*********************** Boundary Specification ***********************!

system      =BDRY ( ( 1-1-1, 1, 1 ) 4 ( 0 ) )

!*********************** Material Assignments ************************!

Ovlmat1    =OVLM ( mod1 / *-*-** / fuel / *-*-*-fuel1, *-*-*-fuel2,
                   *-*-*-fuel3, *-*-*-fuel4, *-*-*-fuel5, *-*-*-fuel6,
                   *-*-*-fuel7, *-*-*-fuel8 / clad / *-*-*-clad )

Omsys1      =OVSM ( Ovlmat1 )

Ovlmat2    =OVLM ( mod2 / *-*-** / Omsys1-Ovlmat1-fuel / 0 /
                   clad / *-*-*-clad )

Ovlmat3    =OVLM ( mod3 / *-*-** / Omsys1-Ovlmat1-fuel / 0 /
                   clad / *-*-*-clad )
```

```
!********************** State Specifications **************************!

Omsys2      =OVSM ( Ovlmat2 )

Omsys3      =OVSM ( Ovlmat3 )

Ovldens     =OVLD ( 1.0 / *-*-** )

Odsys       =OVSD ( Ovldens )

Ovltemp1    =OVLT ( 605.37 / *-*-** / 1200 / *-*-*-fuel1 / 1166 /
                    *-*-*-fuel2 / 1133 / *-*-*-fuel3 / 1100 /
                    *-*-*-fuel4 / 1050 / *-*-*-fuel5 / 1000 /
                    *-*-*-fuel6 / 900 / *-*-*-fuel7 / 750 /
                    *-*-*-fuel8 / 650 / *-*-*-clad )

Ovltemp2    =OVLT ( 582.04 / *-*-** / 1200 / *-*-*-fuel1 / 1166 /
                    *-*-*-fuel2 / 1133 / *-*-*-fuel3 / 1100 /
                    *-*-*-fuel4 / 1050 / *-*-*-fuel5 / 1000 /
                    *-*-*-fuel6 / 900 / *-*-*-fuel7 / 750 /
                    *-*-*-fuel8 / 650 / *-*-*-clad )


Ovltemp3    =OVLT ( 572.04 / *-*-** / 1200 / *-*-*-fuel1 / 1166 /
                    *-*-*-fuel2 / 1133 / *-*-*-fuel3 / 1100 /
                    *-*-*-fuel4 / 1050 / *-*-*-fuel5 / 1000 /
                    *-*-*-fuel6 / 900 / *-*-*-fuel7 /  750 /
                    *-*-*-fuel8 / 650 / *-*-*-clad )

Otsys1      =OVST ( Ovltemp1 )

Otsys2      =OVST ( Ovltemp2 )

Otsys3      =OVST ( Ovltemp3 )

cycle1      =STAT ( Omsys1, Odsys, Otsys1, 137.44 )

cycle2      =STAT ( Omsys2, Odsys, Otsys2, 124.94 )

cycle3      =STAT ( Omsys3, Odsys, Otsys3, 74.96 )

Path        =PATH ( / P, ( cycle1 ), 60 362/55,
                    ( cycle2 ), 115 236/50,
                    ( cycle3 ), 120 736/5, 148 161/14 )

Group       =GROUP ( N / 0 )

Fuel        =AREA ( < *-*-*- ( fuel1, fuel2, fuel3, fuel4, fuel5,
                     fuel6, fuel7, fuel8 ) > )

Pins        =AREA ( *-*-*-< ( fuel1, fuel2, fuel3, fuel4, fuel5,
                     fuel6, fuel7, fuel8 ) > )
```

```
FuelIs      =MICRO ( Group, Fuel / / )

PinIs       =MICRO ( Group, Pins / / )

PinsP       =MACRO ( Group, Pins / bu, kf )

FuelP       =MACRO ( Group, Fuel / bu, kf )

'6p70nf15'   =RUN (  )
```

Information about the format of HELIOS (AURORA) input can be found in reference H-2.

Sample CASMO-3 Input:

```
TIT TFU=1037, TMO=605.37, BOR=750, IDE='burn' *c6p70nf15
PWR, 17, 1.2598, 21.5036        * 17x17 assy, pin pitch
 *
FUE, 1, 6.96/0.219,92238=31.071,94238=0.100,94239=5.221,94240=1.759,
             94241=1.270,94242=0.382,302=35.508,13000=3.581,
             8000=19.258,68166=0.576,68167=0.374,68168=0.437,
             68170=0.244
 *
CAN 5.867
 *
 *
 *
PIN,1,0.409575,0.47498  *no gap                      EMOX FUEL PIN
 *
PIN,2,0.56134,0.60198/'COO','CAN'                      *GUIDE TUBE
 *
 *
PDE 137.44              * POWER DENSITY
 *
 *
PRI,,,,,,,,,,0,              * print #dens at each burnup step
 *
LPI
2
1 1
1 1 1
2 1 1 2
1 1 1 1 1
1 1 1 1 1 2
2 1 1 2 1 1 1
1 1 1 1 1 1 1 1
1 1 1 1 1 1 1 1 1
 *
 *
 *
 *
DEP, -60.362
```

```
STA
 *
TMO=582.04
PDE 124.94
PRI,,,,,,,,,,0,
DEP -115.236
STA
 *
TMO=572.04
PDE 74.96
PRI,,,,,,,,,,0,
DEP -148.161
STA

END
```

Information about the format of CASMO-3 input can be found in reference E-1.

REFERENCES

[A-1] Asou M., Porta J., "Prospects for Poisoning Reactor Cores of the Future", Nuclear Engineering and Design, vol. 168, 1997, pp. 261-270.

[A-2] Albright D., Berkhout F., Walker W., Plutonium and Highly Enriched Uranium 1996 World Inventories, Capabilities and Policies, Stockholm International Peace Research Institute, Oxford University Press, Oxford, UK, 1996.

[B-1] Boltax A., Biancheria A., Chang A. L., Levine P. J., and Lincoln D. K., "Ternary Fuel Performance Data for the Special Water Reactor", WSR-84-252, Westinghouse Electric Corporation, Dec. 1984.

[B-2] Boehm W., et al., "Gd_2O_3 up to 9wt.%, An Established Burnable Poison for Advanced PWRs", Proceedings of the Topical Meeting on Advances in Fuel Management, Pinehurst, Mar. 2-5, 1986.

[B-3] Beard C. A., Buksa J. J., Eaton S. L., Ramsey K. B., "Development of Evolutionary Mixed-Oxide Fuel", Transactions of the American Nuclear Society, vol. 75, Nov., 1996.

[C-1] Chodak P., "Destruction of Plutonium Using Non-Uranium Fuels in Pressurized Water Reactor Peripheral Assemblies", Ph.D. thesis, Massachusetts Institute of Technology, May 1996.

[C-2] Crump M. W., Flynn E. P., "System 80+ Plutonium Disposition Capability", Global '93 International Conference, Seattle WA, Sept. 12-17, 1993.

[C-3] Casal J. J., Stamm'ler R. J. J., Villarino E., Ferri A., "HELIOS: Geometric Capabilities of a New Fuel Assembly Program", Proceedings of the International Topical Meeting on Advances in Mathematics, Computations, and Reactor Physics, CONF-910414, Pittsburgh PA, 1991, Vol. 2, pp. 10.2 1-1 -- 10.2 1.13.

[C-4] Cross Section Evaluation Working Group, "Thermal Reactor Benchmarks Nos. 31-36 (PNL-30 through PNL-35)", Brookhaven National Laboratory, BNL 19302, Nov. 1974, unpublished update Jan. 1981.

[D-1] Driscoll M. J., Downar T. J., Pilat E. E., The Linear Reactivity Model for Nuclear Fuel Management, American Nuclear Society, La Grange Park, IL, 1990, pp 69-73.

[E-1] Edenius M., Forssen B., "CASMO-3, A Fuel Assembly Burnup Program: User's Manual Version 4.7", Studsvik of America Inc., Newton MA, 1993.

[E-2] Eaton S. L., Beard C. A., Buksa J. J., "Evolutionary Mixed-Oxide Fuel Performance in Pressurized Water Reactors", Transactions of the American Nuclear Society, Vol. 75, Nov. 1996.

[F-1] Fisher J. R., Grow R. L., Hodges D., Rapp J. S., Smolinske K. M., "Evaluation of Discrepancies in Assembly Cross Section Generator Codes", Electric Power Research Institute, NP-6147, vols. 1 & 2, 1989.

[G-1] Garcia-Delgado L., "Design of an Economically Optimum PWR Reload Core for a Single-Batch Extended Operating Cycle", S.M. thesis, Massachusetts Institute of Technology, May 1998 (est.).

[H-1] Handwerk, C. S., Meyer J. E., Todreas N. E., "Fuel Performance Analysis of Extended Operating Cycles in Existing LWRs", MIT-NFC-TR-008, Jan. 1998.

[H-2] "HELIOS Documentation", by Scandpower.

[I-1] Ilas D., Rahnema F., "HELIOS Library Benchmark for BWR Analysis", Transactions of the American Nuclear Society, vol. 76, Jun. 1997.

[J-1] Jonsson A., Parrette J. R., Shapiro N. L., "Application of Erbium in Modern Fuel Cycles", ABB-Combustion Engineering, 1991.

[K-1] Kim M., Yoon J., "Conceptual Design for a Deuterium Moderated Pressurized Light Water Cooled Reactor", Proceedings of the American Nuclear Society Topical Meeting on Advances in Nuclear Fuel Management II, Myrtle Beach, SC, Mar. 23-26, 1997.

[L-1] Lindberg M., Piantato C., Gy J.F., "PWR Fuel Design with Erbium as a Burnable Absorber", Proceedings of the American Nuclear Society Topical Meeting on Advances in Nuclear Fuel Management II, Myrtle Beach, SC, Mar. 23-26, 1997.

[M-1] McMahon M. V., Handwerk C. S., MacLean H. J., Driscoll M. J., Todreas N. E., "Modeling and Design of a Reload PWR Core for an Ultra-Long Operating Cycle", MIT-NFC-TR-004, Jul. 1997.

[M-2] Mosteller R. D., Technical Staff Member, Group TSA-10, Los Alamos National Laboratory, personal consultation, Sept. 1996.

[M-3] McMahon M. V., Postdoctoral Associate, Massachusetts Institute of Technology, personal consultation, Nov. 1997.

[N-1] NAS 1994: National Academy of Sciences, Committee on International Security and Arms Control, "Management and Disposition of Excess Weapons Plutonium", National Academy Press, Washington DC.

[O-1] OECD 1995: Organization for Economic Co-operation and Development, Nuclear Energy Agency, Nuclear Science Committee, "Physics of Plutonium Recycling, Volume 1: Issues and Perspectives".

[O-2] Olsen C.S., "Non-Fertile Fuels Development for Plutonium and High-Enriched Uranium Dispositioning in Water Cooled Reactors", Idaho National Engineering Laboratory, Idaho Falls ID, INEL-95/0038, Sept. 1994.

[P-1] Public Service Company of New Hampshire, "Seabrook Station Final Safety Analysis Report", Nov. 1985.

[P-2] Paratte, J.M., Chawla, R., "On the Physics and Feasability of Light Water Reactor Plutonium Fuels Without Uranium", Annals of Nuclear Energy, vol. 7, Jul. 1995.

[S-1] Sterbentz J. W., Olsen C. S., Sinha U. P., "Weapons Grade Plutonium Disposition, Volume 4: Plutonium Dispositioning in Light Water Reactors", DOE/ID-10422, Jun. 1993.

[S-2] Sterbentz J. W., "Neutronic Evaluation of A Non-Fertile Fuel for the Disposition of Weapons-Grade Plutonium in A Boiling Water Reactor", Idaho National Engineering Laboratory, Idaho Falls ID, INEL-94/0079, Oct. 1994.

[S-3] Smith R. I., Konzek G. J., "Clean Critical Experiment Benchmarks for Plutonium Recycle in LWR's", Pacific Northwest Laboratories, Richland WA, NP-196, vol. 1, Apr. 1976.

[Y-1] Yankee Atomic Electric Company, input data for CASMO-3 for modeling a 4-loop Westinghouse PWR, Jul. 1995.